

## GRAVITATIONAL WAVES

Alessandra Buonanno

*Department of Physics, University of Maryland,  
College Park MD 20742, USA  
March 31, 2007*

---

Lectures given at the Fabric of Spacetime Summer School (2006), Les Houches, France.

Photo: width 7.5cm height 11cm

## Contents

1. Introduction	5
2. Linearization of Einstein equations	7
2.1. Einstein equations and gauge symmetry	7
2.2. Wave equation	9
2.3. Transverse-traceless gauge	10
3. Interaction of gravitational waves with point particles	11
3.1. Newtonian and relativistic description of tidal gravity	11
3.2. Description in the transverse-traceless gauge	12
3.3. Description in the free-falling frame	13
3.4. Key ideas underlying gravitational-wave detectors	14
4. Effective stress-energy tensor of gravitational waves	17
5. Generation of gravitational waves	18
5.1. Sources in slow motion, weak-field and negligible self-gravity	18
5.2. Sources in slow motion and weak-field, but non-negligible self-gravity	21
5.3. Radiated energy, angular momentum and linear momentum	22
6. Application to binary systems	23
6.1. Inspiral waveforms at leading Newtonian order	23
6.2. Inspiral waveform including post-Newtonian corrections	26
6.3. Full waveform: inspiral, merger and ring-down	28
6.4. Inspiral templates for data analysis	29
7. Other astrophysical sources	34
7.1. Pulsars	34
7.2. Supernovae	36
8. Cosmological sources	37
8.1. Phenomenological bounds	38
8.2. Gravitational waves produced by causal mechanisms	39
8.3. Gravitational waves produced by cosmic and fundamental strings	41
8.4. Gravitational waves produced during inflation	42
9. Acknowledgments	45
References	45



## 1. Introduction

Gravitational-wave (GW) science has entered a new era. Experimentally <sup>1</sup>, several ground-based laser-interferometer GW detectors (10–1 kHz) have been built in the United States (LIGO) [1], Europe (VIRGO and GEO) [2, 3] and Japan (TAMA) [4], and are now taking data at design sensitivity. Advanced optical configurations capable of reaching sensitivities slightly above and even below the so-called standard-quantum-limit for a *free* test-particle, have been designed for second [5] and third generation [6] GW detectors ( $\sim$  2011–2020). A laser interferometer space antenna (LISA) [7] ( $10^{-4}$ – $10^{-2}$  Hz) might fly within the next decade. Resonant-bar detectors ( $\sim$  1 kHz) [8] are improving more and more their sensitivity, broadening their frequency band. At much lower frequencies,  $\sim 10^{-17}$  Hz, future cosmic microwave background (CMB) probes might *detect* GWs by measuring the CMB polarization [9]. Millisecond pulsar timing can set interesting upper limits [10] in the frequency range  $10^{-9}$ – $10^{-8}$  Hz. At such frequencies, the large number of millisecond pulsars which will be detectable with the square kilometer array [11], would provide an ensemble of clocks that can be used as multiple arms of a GW detector.

Theoretically, the last years have been characterized by numerous major advances. For what concerns the most promising GW sources for ground-based and space-based detectors, notably, binary systems composed of neutron stars (NS) and black holes (BHs), our understanding of the two-body problem and the GW-generation problem has improved significantly. The best-developed *analytic* approximation method in general relativity is undoubtedly the post-Newtonian (PN) method. The errors and ambiguities that characterized the very early literature on the PN problem of motion (for a review see, e.g., Ref. [12]), have been overcome. Robust predictions are currently available through 3.5PN order [13] ( $v^7/c^7$ ), if the compact objects do not carry spin, and 2.5PN order [15] ( $v^5/c^5$ ) if they carry spin. Resummation of the PN expansion aimed at pushing analytic calculations until the final stage of evolution, including the transition inspiral–merger–ring-down, have also been proposed, for the conservative two-body dynamics [16] and the radiation-reaction effects [17]. Quite interestingly, the effective-field-theory approach, commonly used in particle physics, has been extended to gravity, no-

---

<sup>1</sup>GW experiments started with the pioneering work of Joseph Weber at Maryland in the 60s

tably to the two-body problem of motion [18]. The recent dazzling breakthrough in *numerical relativity* [19], with different independent groups being able to successfully evolve a comparable-mass BH binary throughout inspiral, merger and ring-down and extract the GW signal, is allowing to dig out details of the nonlinear dynamics which could not be *fully* predicted with other means.

Our knowledge has also progressed on the problem of motion of a point particle in curved spacetime when the emission of GWs is taken into account (non-geodesic motion) [20, 21]. To solve this problem is of considerable importance for predicting very accurate waveforms emitted by extreme mass-ratio binaries, which are among the most promising sources for LISA [22].

The GW community working at the interface between the theory and the experiment has provided *templates* [16, 17, 23] for binaries and developed robust algorithms [24, 25] for pulsars and other GW sources observable with ground-based and space-based interferometers. The joined work of data analysts and experimentalists has established astrophysically significant upper limits for several GW sources [26–28] and is now eagerly waiting for the first detection.

These lectures were envisioned to be an introductory, basic course in GW theory. Many of the topics that we shall address are thoroughly discussed in several books [29–35] and proceedings or reviews [36–42]. The lectures focused more on binary systems, probably because biased towards the author own background and expertise. The lectures are organized as follows. In Sec. 2 we start by deriving the wave equation in linearized gravity and discuss the main properties of GWs. In Sec. 3 we describe the interaction of GWs with free test particles and the key ideas underlying the functioning of GW detectors. Section 4 reviews the effective stress-energy tensor of GWs. Section 5 is devoted to the generation problem. We explicitly derive the gravitational field at leading order assuming slow-motion, weak-gravity and negligible self-gravity. We then discuss how those results can be extended to non-negligible self-gravity sources. As a first application, in Sec. 6 we compute the GW signal from binary systems. We discuss briefly the state-of-the-art of PN calculations and NR results. As an example of data-analysis issues, we compute the GW templates in the stationary-phase-approximation (SPA). In Sec. 7 we apply the results of Sec. 6 to other astrophysical sources, notably pulsars and supernovae. Section 8 focus on cosmological sources at much higher red-shift  $z \gg 1$ . We review the main physical mechanisms that could have produced GWs in the early Universe, notably first-order phase transitions, cosmic and fundamental strings, and inflation.

## 2. Linearization of Einstein equations

In 1916 Einstein realized the propagation effects at finite velocity in the gravitational equations and predicted the existence of wave-like solutions of the linearized vacuum field equations [43]. In this section we expand Einstein equations around the flat Minkowski metric derive the wave equation and put the solution in a simple form using an appropriate gauge.

### 2.1. Einstein equations and gauge symmetry

The Einstein action reads

$$S_g = \frac{c^3}{16\pi G} \int d^4x \sqrt{-g} R, \quad (2.1)$$

where  $c$  denotes the speed of light,  $G$  the Newton constant,  $g_{\mu\nu}$  is the four dimensional metric and  $g = \det(g_{\mu\nu})$ . Henceforth, we use the following conventions. The flat Minkowski metric is  $\eta_{\mu\nu} = (-, +, +, +)$ , Greek indices denote spacetime coordinates  $\mu, \nu = 0, 1, 2, 3$ , whereas Latin indices denote spacelike coordinates  $i, j = 1, 2, 3$ . Moreover,  $x^\mu = (x^0, \mathbf{x}) = (ct, \mathbf{x})$ , thus  $d^4x = c dt d^3x$ . Partial derivatives  $\partial_\mu$  will be denoted with a comma, while covariant derivatives with a semicolon. The scalar tensor  $R$  in Eq. (2.1) is obtained from the curvature tensor as

$$R = g^{\mu\nu} R_{\mu\nu}, \quad R_{\mu\nu} = g^{\rho\sigma} R_{\rho\mu\sigma\nu}, \quad (2.2)$$

$$R^\nu{}_{\mu\rho\sigma} = \frac{\partial \Gamma^\nu{}_{\mu\sigma}}{\partial x^\rho} - \frac{\partial \Gamma^\nu{}_{\mu\rho}}{\partial x^\sigma} + \Gamma^\nu{}_{\lambda\rho} \Gamma^\lambda{}_{\mu\sigma} - \Gamma^\nu{}_{\lambda\sigma} \Gamma^\lambda{}_{\mu\rho}, \quad (2.3)$$

where  $\Gamma^\nu{}_{\mu\sigma}$  are the affine connections

$$\Gamma^\mu{}_{\nu\rho} = \frac{1}{2} g^{\mu\lambda} \left( \frac{\partial g_{\lambda\nu}}{\partial x^\rho} + \frac{\partial g_{\lambda\rho}}{\partial x^\nu} - \frac{\partial g_{\nu\rho}}{\partial x^\lambda} \right). \quad (2.4)$$

The curvature tensor satisfies the following properties

$$R_{\mu\nu\rho\sigma} = -R_{\nu\mu\rho\sigma} = -R_{\mu\nu\sigma\rho}, \quad R_{\mu\nu\rho\sigma} = R_{\rho\sigma\mu\nu}, \quad (2.5)$$

$$R_{\mu\nu\rho\sigma} + R_{\mu\sigma\nu\rho} + R_{\mu\rho\sigma\nu} = 0, \quad R^\lambda{}_{\mu\nu\rho;\sigma} + R^\lambda{}_{\mu\sigma\nu;\rho} + R^\lambda{}_{\mu\rho\sigma;\nu} = 0. \quad (2.6)$$

The latter equation is known as the Bianchi identity. We define the matter energy-momentum tensor  $T_{\mu\nu}$  from the variation of the matter action  $S_m$  under a change of the metric  $g_{\mu\nu} \rightarrow g_{\mu\nu} + \delta g_{\mu\nu}$ , that is

$$\delta S_m = \frac{1}{2c} \int d^4x \sqrt{-g} T^{\mu\nu} \delta g_{\mu\nu}. \quad (2.7)$$

The variation of the total action  $S = S_g + S_m$  with respect to  $g_{\mu\nu}$  gives the Einstein equations

$$G_{\mu\nu} = R_{\mu\nu} - \frac{1}{2} g_{\mu\nu} R = \frac{8\pi G}{c^4} T_{\mu\nu}. \quad (2.8)$$

The above equations are nonlinear equations with well posed initial value structure, i.e. they determine future values of  $g_{\mu\nu}$  from given initial values. Since  $\mu = 0, \dots, 3, \nu = 0, \dots, 3$ , Eq. (2.8) contains sixteen differential equations, which reduce to ten differential equations if the symmetry of the tensors  $G_{\mu\nu}$  and  $T_{\mu\nu}$  is used. Finally, because of the Bianchi identity we have  $G_{\mu\nu}{}^{;\nu} = 0$ , thus the ten differential equations reduce to six.

General relativity is invariant under the group of all possible coordinate transformations

$$x^\mu \rightarrow x'^\mu(x), \quad (2.9)$$

where  $x'^\mu$  is invertible, differentiable and with a differentiable inverse. Under the above transformation, the metric transforms as

$$g_{\mu\nu}(x) \rightarrow g'_{\mu\nu}(x') = \frac{\partial x^\rho}{\partial x'^\mu} \frac{\partial x^\sigma}{\partial x'^\nu} g_{\rho\sigma}(x). \quad (2.10)$$

We assume that there exists a reference frame in which, on a sufficiently large spacetime region, we can write

$$g_{\mu\nu} = \eta_{\mu\nu} + h_{\mu\nu}, \quad |h_{\mu\nu}| \ll 1. \quad (2.11)$$

By choosing this particular reference frame, we break the invariance of general relativity under coordinate transformations. However, a residual gauge symmetry remains. Let us consider the following coordinate transformation

$$x^\mu \rightarrow x'^\mu = x^\mu + \xi^\mu(x), \quad |\partial_\mu \xi_\nu| \leq |h_{\mu\nu}|. \quad (2.12)$$

The metric transforms as

$$g'_{\mu\nu} = \eta_{\mu\nu} - \partial_\nu \xi_\mu - \partial_\mu \xi_\nu + h_{\mu\nu} + \mathcal{O}(\partial\xi^2), \quad (2.13)$$

thus, introducing

$$h'_{\mu\nu} = h_{\mu\nu} - \xi_{\mu,\nu} - \xi_{\nu,\mu}, \quad (2.14)$$

we have

$$g'_{\mu\nu} = \eta_{\mu\nu} + h'_{\mu\nu}, \quad |h'_{\mu\nu}| \ll 1. \quad (2.15)$$

In conclusion, the slowly varying coordinate transformations (2.12) are a symmetry of the linearized theory. Under a finite, global ( $x$ -independent) Lorentz transformation

$$x^\mu \rightarrow \Lambda_\nu^\mu x^\nu, \quad \Lambda_\mu^\rho \Lambda_\nu^\sigma \eta_{\rho\sigma} = \eta_{\mu\nu}, \quad (2.16)$$



the metric transforms as

$$g_{\mu\nu} \rightarrow g'_{\mu\nu}(x') = \Lambda_\mu^\rho \Lambda_\nu^\sigma g_{\rho\sigma} = \eta_{\mu\nu} + \Lambda_\mu^\rho \Lambda_\nu^\sigma h_{\rho\sigma}(x) = \eta_{\mu\nu} + h'_{\mu\nu}(x'), \quad (2.17)$$

thus,  $h_{\mu\nu}$  is a tensor under Lorentz transformations. It is straightforward to prove that  $h_{\mu\nu}$  is also invariant under translations. In conclusions, linearized theory is invariant under the Poincaré group and under the transformation  $x^\mu \rightarrow x^\mu + \xi^\mu$  with  $|\partial_\nu \xi^\mu| \ll 1$ .

## 2.2. Wave equation

Let us now linearize Einstein equations posing  $g_{\mu\nu} = \eta_{\mu\nu} + h_{\mu\nu}$ . At linear order in  $h_{\mu\nu}$  the affine connections and curvature tensor read

$$\Gamma_{\mu\rho}^\nu = \frac{1}{2} \eta^{\nu\lambda} (\partial_\rho h_{\lambda\mu} + \partial_\mu h_{\lambda\rho} - \partial_\lambda h_{\mu\rho}), \quad (2.18)$$

$$R_{\mu\rho\sigma}^\nu = \partial_\rho \Gamma_{\mu\sigma}^\nu - \partial_\sigma \Gamma_{\mu\rho}^\nu + \mathcal{O}(h^2), \quad (2.19)$$

more explicitly

$$R_{\mu\nu\rho\sigma} = \frac{1}{2} (\partial_{\rho\nu} h_{\mu\sigma} + \partial_{\sigma\mu} h_{\nu\rho} - \partial_{\rho\mu} h_{\nu\sigma} - \partial_{\sigma\nu} h_{\mu\rho}). \quad (2.20)$$

Using the above equations, it is straightforward to show that the linearized Riemann tensor is invariant under the transformation  $h_{\mu\nu} \rightarrow h_{\mu\nu} - \partial_\mu \xi_\nu - \partial_\nu \xi_\mu$ . Equation (2.20) can be greatly simplified if we introduce the so-called *trace-reverse* tensor

$$\bar{h}^{\mu\nu} = h^{\mu\nu} - \frac{1}{2} \eta^{\mu\nu} h, \quad (2.21)$$

where  $h = \eta_{\alpha\beta} h^{\alpha\beta}$  and  $\bar{h} = -h$ , which explains the name. Some algebra leads to

$$\square \bar{h}_{\nu\sigma} + \eta_{\nu\sigma} \partial^\rho \partial^\lambda \bar{h}_{\rho\lambda} - \partial^\rho \partial_\nu \bar{h}_{\rho\sigma} - \partial^\rho \partial_\sigma \bar{h}_{\rho\nu} + \mathcal{O}(h^2) = -\frac{16\pi G}{c^4} T_{\nu\sigma}, \quad (2.22)$$

where the wave operator  $\square = \eta_{\rho\sigma} \partial^\rho \partial^\sigma$ . To further simplify Eq. (2.22) we can impose the Lorenz gauge (also denoted in the literature as harmonic or De Donder gauge)

$$\partial_\nu \bar{h}^{\mu\nu} = 0, \quad (2.23)$$

and obtain

$$\square \bar{h}_{\nu\sigma} = -\frac{16\pi G}{c^4} T_{\nu\sigma}. \quad (2.24)$$

If  $\bar{h}^{\mu\nu}$  does not satisfy the Lorenz gauge, i.e.  $\partial_\mu \bar{h}^{\mu\nu} = q_\nu$ , we can introduce a coordinate transformation such that  $\bar{h}'_{\mu\nu} = \bar{h}_{\mu\nu} - \xi_{\mu,\nu} - \xi_{\nu,\mu} + \eta_{\mu\nu} (\partial_\rho \xi^\rho)$  and impose  $\square \xi_\nu = q_\nu$ , obtaining  $\partial_\mu \bar{h}'^{\mu\nu} = 0$ .

Summarizing, the Lorenz gauge imposes 4 conditions that allow to reduce the 10 independent components of the  $4 \times 4$  symmetric tensor  $h_{\mu\nu}$  to 6 independent components. Note that we also have the condition  $\partial_\mu T^{\mu\nu} = 0$ , which is the conservation of the energy-momentum tensor of the matter in linearized theory. By contrast in the full theory  $T^{\mu\nu}_{;\nu} = 0$ .

### 2.3. Transverse-traceless gauge

We want to study the propagation of GWs once they have been generated. We set  $T_{\mu\nu} = 0$  in Eq. (2.24) and obtain the wave equation in vacuum

$$\square \bar{h}_{\mu\nu} = 0. \quad (2.25)$$

GWs propagate at the speed of light. Within the Lorenz gauge we can always consider coordinate transformations such that  $\square \xi_\mu = 0$ . The trace-reverse tensor transforms as  $\bar{h}'_{\mu\nu} = \bar{h}_{\mu\nu} + \xi_{\mu\nu}$  with  $\xi_{\mu\nu} = \eta_{\mu\nu} \partial_\rho \xi^\rho - \xi_{\mu,\nu} - \xi_{\nu,\mu}$ . Using  $\square \xi_{\mu\nu} = 0$ , we can subtract 4 of the 6 components of  $\bar{h}_{\mu\nu}$ . More specifically, we can choose  $\xi^0$  such that  $\bar{h} = 0$  and  $\xi^i$  such that  $h^{i0} = 0$ , thus  $\partial_0 h^{00} = 0$ . The GW being a time-dependent field, we can set  $h^{00} = 0$ . We denote the field  $h_{ij}$  which satisfies the following transverse and traceless gauge conditions,

$$h^{00} = 0, \quad h^{0i} = 0, \quad \partial_i h^{ij} = 0, \quad h^{ii} = 0, \quad (2.26)$$

the *transverse-traceless* tensor  $h_{ij}^{\text{TT}}$ . Note that for a single plane wave with wave vector  $\mathbf{k}$  and propagation direction  $\mathbf{n} = \mathbf{k}/k$ , the transversality condition reduces to  $n^i h_{ij}^{\text{TT}} = 0$ . Without losing in generality, we can assume that the plane wave propagates along the  $z$ -axis, thus

$$h_{ij}^{\text{TT}}(t, z) = \begin{pmatrix} h_+ & h_\times & 0 \\ h_\times & -h_+ & 0 \\ 0 & 0 & 0 \end{pmatrix} \cos \left[ \omega \left( t - \frac{z}{c} \right) \right], \quad (2.27)$$

where we indicate with  $h_+$  and  $h_\times$  the two independent polarization states. Following [31, 35], we can introduce the projector operator  $P_{ij}(\mathbf{n}) = \delta_{ij} - n_i n_j$ , which satisfies the conditions

$$P_{ij} = P_{ji}, \quad n^i P_{ij} = 0, \quad P_{ij} P^{jk} = P_i^k, \quad P_{ii} = 2, \quad (2.28)$$

and the  $\Lambda$ -operator

$$\Lambda_{ij\,kl}(\mathbf{n}) = P_{ik} P_{jl} - \frac{1}{2} P_{ij} P_{kl}, \quad (2.29)$$

and obtain the TT field for a generic propagation direction

$$h_{ij}^{\text{TT}} = \Lambda_{ij,kl} h_{kl}, \quad (2.30)$$

where  $h_{kl}$  is given in the Lorenz gauge but not necessarily in the TT gauge.

The GW is described in the TT gauge by a  $2 \times 2$  matrix in the plane orthogonal to the direction of propagation  $\mathbf{n}$ . If we perform a rotation  $\psi$  about the axis  $\mathbf{n}$ , we obtain

$$h_{\times} \pm i h_{+} \rightarrow e^{\mp 2i\psi} (h_{\times} \pm i h_{+}). \quad (2.31)$$

In particle physics we call helicity the projection of the (total) angular momentum along the propagation direction:  $\mathcal{H} = \mathbf{J} \cdot \mathbf{n} = \mathbf{S} \cdot \mathbf{n}$ , being  $\mathbf{S}$  the particle's spin. Under a rotation  $\psi$  about the propagation direction the helicity states transform as  $h \rightarrow e^{i\mathcal{H}\psi} h$ . Thus, Eq. (2.31) states that  $h_{\times} - i h_{+}$  are the helicity states and that the graviton is a spin-2 particle.

### 3. Interaction of gravitational waves with point particles

#### 3.1. Newtonian and relativistic description of tidal gravity

Let us consider two point particles, labeled A and B, falling freely through 3-D Euclidean space under the action of an external Newtonian potential  $\Phi$ . We assume that at time  $t = 0$  the particles are separated by a small distance  $\xi$  and have initially the same speed  $\mathbf{v}_A(t = 0) = \mathbf{v}_B(t = 0)$ . Since the two particles are at slightly different positions, they experience a slightly different gravitational potential  $\Phi$  and a different acceleration  $\mathbf{g} = -\nabla\Phi$ . At time  $t > 0$ ,  $\mathbf{v}_A(t) \neq \mathbf{v}_B(t)$ . Let us introduce the separation vector  $\xi = \mathbf{x}_A - \mathbf{x}_B$  in 3-D Euclidean space. We have

$$\frac{d^2 \xi^i}{dt^2} = - \left( \frac{\partial \Phi}{\partial x^i} \right)_B + \left( \frac{\partial \Phi}{\partial x^i} \right)_A \simeq - \left( \frac{\partial^2 \Phi}{\partial x^i \partial x^j} \right) \xi^j \equiv \mathcal{E}_j^i \xi^j, \quad (3.1)$$

where the second equality is obtained by Taylor expanding around the position of particle A. The tensor  $\mathcal{E}_j^i$  is called the *Newtonian tidal-gravity* tensor [42], it measures the inhomogeneities of Newtonian gravity. It is the tensor responsible of the Moon's tides on the Earth's ocean.

We now generalize the above Newtonian discussion to Einstein theory. In general relativity, nonspinning test particles move along geodesics

$$\frac{d^2 x^\mu}{d\tau^2} + \Gamma_{\rho\sigma}^\mu(x) \frac{dx^\rho}{d\tau} \frac{dx^\sigma}{d\tau} = 0, \quad (3.2)$$

where  $\Gamma_{\rho\sigma}^\mu(x)$  is given by Eq. (2.19). Let us consider two nearby geodesics, labeled A and B, parametrized by  $x^\mu(\tau)$  and  $x^\mu(\tau) + \xi^\mu(\tau)$ , with  $|\xi^\mu|$  smaller than the typical scale on which the gravitational field varies. By expanding the

geodesic equation of particle B around the position of particle A, and subtracting it from the geodesic equation of particle A, we get

$$\nabla_u \nabla_u \xi^\mu = -R^\mu{}_{\nu\rho\sigma} \xi^\rho \frac{dx^\nu}{d\tau} \frac{dx^\sigma}{d\tau}, \quad (3.3)$$

$u^\beta = dx^\beta/d\tau$  being the four-velocity and where we introduce the covariant derivative along the curve  $x^\mu(\tau)$

$$\nabla_u \xi^\mu = \frac{d\xi^\mu}{d\tau} + \Gamma^\mu{}_{\rho\sigma} \xi^\rho \frac{dx^\sigma}{d\tau}. \quad (3.4)$$

Thus, two nearby time-like geodesics experience a tidal gravitational *force* proportional to the Riemann tensor.

### 3.2. Description in the transverse-traceless gauge

In this section we describe the interaction of a GW with a point particle in the TT gauge. Let us consider a test particle A at rest at time  $\tau = 0$ . Using the geodesic equation, we have

$$\frac{d^2 x^i}{d\tau^2} \Big|_{\tau=0} = - \left( \Gamma^i{}_{\rho\sigma} \frac{dx^\rho}{d\tau} \frac{dx^\sigma}{d\tau} \right) \Big|_{\tau=0} = - \left( \Gamma^i{}_{00} \frac{dx^0}{d\tau} \frac{dx^0}{d\tau} \right) \Big|_{\tau=0}. \quad (3.5)$$

Because the particle is initially at rest  $(dx^\mu/d\tau)_{\tau=0} = (c, 0)$  and

$$\Gamma^i{}_{00} = \frac{1}{2} \eta^{ij} (\partial_0 h_{0j} + \partial_0 h_{j0} - \partial_j h_{00}). \quad (3.6)$$

In the TT gauge  $h_{00} = 0$  and  $h_{0j} = 0$ , so  $(\Gamma^i{}_{00})_{\tau=0} = 0$ . Thus, we conclude that in the TT gauge, if at time  $\tau = 0$ ,  $dx^i/d\tau = 0$ , also  $d^2 x^i/d\tau^2 = 0$  and a particle at rest before the GW arrives, remains at rest. The coordinates in the TT gauge stretch themselves when the GW arrives so that the coordinate position of the point particles, initially at rest, does not vary. What varies is the proper distance between the two particles and physical effects are monitored by proper distances.

For a wave propagating along the  $z$ -axis, the metric is [see Eq. (2.27)]

$$ds^2 = -c^2 dt^2 + dz^2 + dy^2 \left[ 1 - h_+ \cos \omega \left( t - \frac{z}{c} \right) \right] + dx^2 \left[ 1 + h_+ \cos \omega \left( t - \frac{z}{c} \right) \right] + 2dx dy h_\times \cos \omega \left( t - \frac{z}{c} \right). \quad (3.7)$$

If particles A and B set down initially along the  $x$ -axis, we have

$$s \simeq L \left( 1 + \frac{h_+}{2} \cos \omega t \right), \quad (3.8)$$

where  $L$  is the initial, unperturbed distance between particles A and B.

### 3.3. Description in the free-falling frame

It is always possible to perform a change of coordinates such that at a given space-time point  $\mathcal{Q}$ , we can set  $\Gamma_{\rho\sigma}^{\mu}(\mathcal{Q}) = 0$  and  $(d^2x^{\mu}/d\tau^2)_{\mathcal{Q}} = 0$ . In this frame, at one moment in space and one moment in time, the point particle is *free falling* (FF). This frame can be explicitly constructed using *Riemann normal coordinates* [30]. Actually, it is possible to build a frame such that the point particle is free-falling all along the geodesics using *Fermi normal coordinates* [30].

Let us introduce a FF frame attached to particle A with spatial origin at  $x^j = 0$  and coordinate time equal to proper time  $x^0 = \tau$ . By definition of a FF frame, the metric reduces to Minkowski metric at the origin and all its derivatives vanish at the origin, that is

$$ds^2 = -c^2 dt^2 + dx^2 + \mathcal{O}\left(\frac{|\mathbf{x}|^2}{\mathcal{R}^2}\right), \quad (3.9)$$

where  $\mathcal{R}$  is the curvature radius  $\mathcal{R}^{-2} = |R_{\mu\nu\rho\sigma}|$ . Doing explicitly the calculation at second order in  $x$ , one finds [44]

$$\begin{aligned} ds^2 = & -c^2 dt^2 [1 + R_{i0j0} x^i x^j] - 2c dt dx^i \left(\frac{2}{3} R_{0jik} x^j x^k\right) + \\ & dx^i dx^j \left[\delta_{ij} - \frac{1}{3} R_{ijkl} x^k x^l\right]. \end{aligned} \quad (3.10)$$

For GW experiments located on the Earth, the interferometer is not in free fall with respect to the Earth gravity. The detector is subjected to an acceleration  $\mathbf{a} = -\mathbf{g}$  with respect to a local inertial frame and it rotates with respect to local gyroscopes. Thus, in general the effect of GWs on point particles compete with other effects. We shall restrict our discussion to the frequency band (10–10<sup>3</sup> Hz) in which the other effects are subdominant and/or static.

Let us compute the equation of geodesic deviation in the FF frame attached to particle A. We have

$$\nabla_u \nabla_u \xi^\alpha = u^\beta \nabla_\beta (u^\lambda \nabla_\lambda \xi^\alpha) = u^\beta u^\lambda (\partial_{\beta\lambda} \xi^\alpha + \Gamma_{\lambda\sigma,\beta}^\alpha \xi^\sigma), \quad (3.11)$$

where in the last equality we use  $\Gamma_{\lambda\sigma}^\alpha = 0$ . Since we assume that the particles are initially at rest,  $u^\beta = \delta_0^\beta$ . Using  $\xi^0 = 0$  and the fact that  $\Gamma_{0k,0}^j$  can be neglected when computed at position A, we have

$$\nabla_u \nabla_u \xi^j = \frac{d^2 \xi^j}{d\tau^2} \Rightarrow \frac{d^2 \xi^j}{d\tau^2} = -R_{0k0}^j \xi^k. \quad (3.12)$$

To complete the calculation we need to evaluate the Riemann tensor  $R_{0k0}^j$ . As discussed in Sec. 2.2, in linearized theory the Riemann tensor is invariant under

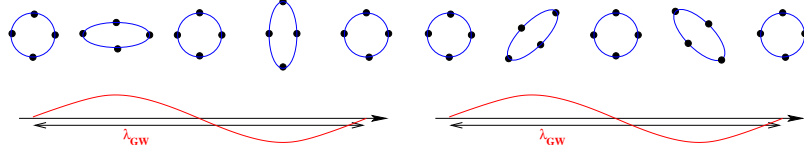


Fig. 1. We show how point particles along a ring move as a result of the interaction with a GW propagating in the direction perpendicular to the plane of the ring. The left panel refers to a wave with + polarization, the right panel with  $\times$  polarization.

change of coordinates, so we can compute it in the TT gauge. Using Eq. (2.20), we obtain

$$R_{j0k0}^{\text{TT}} = -\frac{1}{2c^2} \ddot{h}_{jk}^{\text{TT}}. \quad (3.13)$$

Thus,

$$\frac{d^2 \xi^j}{dt^2} = \frac{1}{2} \ddot{h}_{jk}^{\text{TT}} \xi^k. \quad (3.14)$$

In conclusion, in the FF frame the effect of a GW on a point particle of mass  $m$  can be described in terms of a *Newtonian force*  $F_i = (m/2) \ddot{h}_{ij}^{\text{TT}} \xi^j$ . Note that in the FF frame, coordinate distances and proper distances coincide, and we recover immediately Eq. (3.8).

The description in the FF frame is useful and simple as long as we can write the metric as  $g_{\mu\nu} = \eta_{\mu\nu} + \mathcal{O}(x^2/\mathcal{R}^2)$ , i.e. as long as we can disregard the corrections  $x^2/\mathcal{R}^2$ . Since  $\mathcal{R}^{-2} = |R_{i0j0}| \sim \ddot{h} \sim h/\lambda_{\text{GW}}^2$ , we have  $x^2/\mathcal{R}^2 \simeq L^2 h/\lambda_{\text{GW}}^2$ , and comparing it with  $\delta L/L \sim h$ , we find  $L^2/\lambda_{\text{GW}}^2 \ll 1$ . This condition is satisfied by ground-based detectors because  $L \sim 4$  km and  $\lambda_{\text{GW}} \sim 3000$  km, but not by space-based detectors which have  $L \sim 5 \times 10^6$  km and will observe GWs with wavelength shorter than  $L$ . [For a recent thorough analysis and a proof of the equivalence between the TT and FF description, see, e.g., Ref. [45].]

### 3.4. Key ideas underlying gravitational-wave detectors

To illustrate the effect of GWs on FF particles, we consider a ring of point particles initially at rest with respect to a FF frame attached to the center of the ring, as shown in Fig. 1. We determine the motion of the particles considering the + and  $\times$  polarizations separately. If only the + polarization is present, we have

$$h_{ij}^{\text{TT}} = h_+ \begin{pmatrix} 1 & 0 \\ 0 & -1 \end{pmatrix} \sin \omega t, \quad \xi_i = [x_0 + \delta x(t), y_0 + \delta y(t)], \quad (3.15)$$

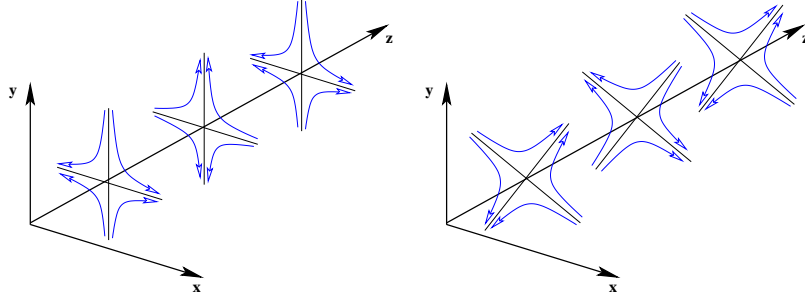


Fig. 2. Lines of force associated to the + (left panel) and  $\times$  (right panel) polarizations.

where  $x_0$  and  $y_0$  are the unperturbed position at time  $t = 0$ . Thus

$$\delta x(t) = \frac{h_+}{2} x_0 \sin \omega t \quad \delta y(t) = -\frac{h_+}{2} y_0 \sin \omega t. \quad (3.16)$$

If only the  $x$  polarization is present, a straightforward calculation gives

$$\delta x(t) = \frac{h_\times}{2} y_0 \sin \omega t \quad \delta y(t) = \frac{h_\times}{2} x_0 \sin \omega t. \quad (3.17)$$

The + and  $\times$  polarizations differ by a rotation of  $45^\circ$ . In Fig. 2 we show the lines of force associated to the + and  $\times$  polarizations.

The simplest GW detector we can imagine is a body of mass  $m$  at a distance  $L$  from a fiducial laboratory point, connected to it by a spring of resonant frequency  $\Omega$  and quality factor  $Q$ . Einstein equation of geodesic deviation predicts that the infinitesimal displacement  $\Delta L$  of the mass along the line of separation from its equilibrium position satisfies the equation [36] (valid for wavelengths  $\gg L$  and in the FF frame of the observer at the fiducial laboratory point)

$$\ddot{\Delta L}(t) + 2\frac{\Omega}{Q} \dot{\Delta L}(t) + \Omega^2 \Delta L(t) = \frac{L}{2} [F_+ \ddot{h}_+(t) + F_\times \ddot{h}_\times(t)], \quad (3.18)$$

where  $F_{+,\times}$  are coefficients of order unity which depend on the direction of the source [see Eqs. (6.31), (6.31) below] and the GW polarization angle.

Laser-interferometer GW detectors are composed of two perpendicular km-scale arm cavities with two test-mass mirrors hung by wires at the end of each cavity. The tiny displacements  $\Delta L$  of the mirrors induced by a passing GW are monitored with very high accuracy by measuring the relative optical phase between the light paths in each interferometer arm. The mirrors are pendula with quality factor  $Q$  quite high and resonant frequency  $\Omega$  much lower ( $\sim 1$  Hz) than

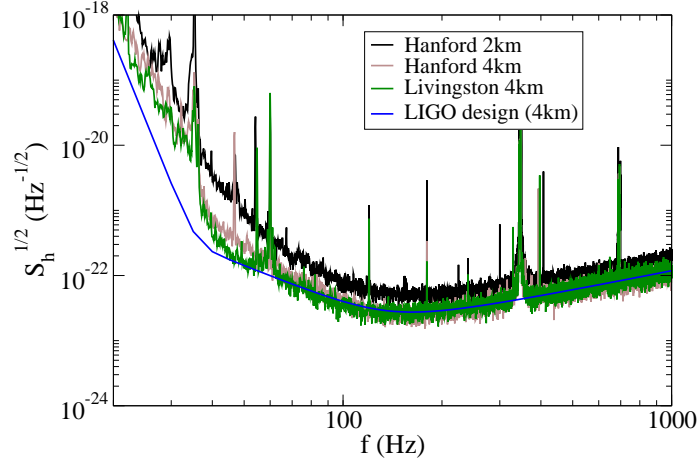


Fig. 3. We plot the square root of the noise spectral density versus frequency for the three LIGO detectors together with the LIGO noise curve at designed sensitivity. The noise curves refer to June 2006, during the fifth scientific run.

the typical GW frequency ( $\sim 100$  Hz). In this case Eq. (3.18), written in Fourier domain, reduces to  $\Delta L/L \sim h$ . The typical amplitude, at 100 Hz, of GWs emitted by binary systems in the VIRGO cluster of galaxies ( $\sim 20$  Mpc distant), which is the largest distance the first-generation ground-based interferometers can probe, is  $\sim 10^{-21}$ . This means  $\Delta L \sim 10^{-18}$  m, a very tiny number. It may appear rather discouraging, especially if we think to monitor the test-mass motion with light of wavelength nearly  $10^{12}$  times larger. However, this precision is currently being demonstrated experimentally.

The electromagnetic signal leaking out the interferometer's dark-port contains the GW signal but also noise — for example the thermal noise from the suspension system and the mirror itself, can shake the mirror mimicking the effect of a GW. The root-mean-square of the noise is generally expressed in terms of the noise power per unit frequency  $S_h$  through the relation  $h \sim \sqrt{S_h(f) \Delta f} \sim \Delta L/L$ ,  $\Delta L$  being the mirror displacement induced by noise and  $\Delta f$  the frequency bandwidth. In Fig. 3 we plot the noise curves of LIGOs (June 2006). The interferometers are currently operating at design sensitivity for almost the entire frequency band.



#### 4. Effective stress-energy tensor of gravitational waves

Until now we have defined the GWs as fluctuations of a flat spacetime. Here, we want to be more general and consider GWs as perturbations of a generic background  $\bar{g}_{\mu\nu}$ , that is

$$g_{\mu\nu} = \bar{g}_{\mu\nu} + h_{\mu\nu}, \quad |h_{\mu\nu}| \ll 1. \quad (4.1)$$

We need a criterion to define what is the background and what is the perturbation. Henceforth, we follow closely the derivation in Ref. [35]. In general there are two cases:

1.  $\bar{g}_{\mu\nu}$  has typical scale  $L_B$  and  $h_{\mu\nu}$  has typical wavelength  $\lambda$  with  $\lambda \ll L_B$ , i.e.  $h_{\mu\nu}$  is a small *ripple* on a smooth background;
2.  $\bar{g}_{\mu\nu}$  has frequencies only up to  $f_B$  and  $h_{\mu\nu}$  is different from zero around  $f$  with  $f \gg f_B$ , i.e. the background is static.

Let us expand  $R_{\mu\nu}$  through  $\mathcal{O}(h^2)$ . Note that we have now two small parameters  $h$  and  $\lambda/L_B$  (or  $f_B/f$ ), we have

$$R_{\mu\nu} = \underbrace{\bar{R}_{\mu\nu}}_{\text{low freq}} + \underbrace{R_{\mu\nu}^{(1)}}_{\text{high freq}} + \underbrace{R_{\mu\nu}^{(2)}}_{\text{low and high freq}} + \dots \quad (4.2)$$

Quantities having a bar are computed using the background metric  $\bar{g}_{\mu\nu}$ ; they contain only low-frequency modes. The superscript (1) [(2)] in Eq. (4.2) refers to quantities computed at linear (quadratic) order in  $h$ . Using the Einstein equations we get

$$\bar{R}_{\mu\nu} = -[R_{\mu\nu}^{(2)}]_{\text{low freq}} + \frac{8\pi G}{c^4} \left[ T_{\mu\nu} - \frac{1}{2} g_{\mu\nu} T \right]_{\text{low freq}}. \quad (4.3)$$

We introduce a scale  $\ell$  such that  $\lambda \ll \ell \ll L_B$ , and average over a spatial volume  $\ell^3$  [35, 46]. We denote the average as  $\langle \rangle$ . Short-wave modes average to zero, whereas modes with wavelength  $L_B$  are constant. We can rewrite Eq. (4.3) as

$$\begin{aligned} \bar{R}_{\mu\nu} &= -\langle R_{\mu\nu}^{(2)} \rangle + \frac{8\pi G}{c^4} \langle T_{\mu\nu} - \frac{1}{2} g_{\mu\nu} T \rangle \\ &\equiv -\langle R_{\mu\nu}^{(2)} \rangle + \frac{8\pi G}{c^4} \left( \bar{T}_{\mu\nu} - \frac{1}{2} \bar{g}_{\mu\nu} \bar{T} \right). \end{aligned} \quad (4.4)$$

Defining the *effective* stress-energy tensor of GWs

$$t_{\mu\nu} = -\frac{c^4}{8\pi G} \langle R_{\mu\nu}^{(2)} - \frac{1}{2} \bar{g}_{\mu\nu} R^{(2)} \rangle, \quad (4.5)$$

we have

$$\bar{R}_{\mu\nu} - \frac{1}{2}\bar{g}_{\mu\nu}\bar{R} = \frac{8\pi G}{c^4}(\bar{T}_{\mu\nu} + t_{\mu\nu}). \quad (4.6)$$

An explicit calculation carried on far from the source gives

$$t_{\mu\nu} = \frac{c^4}{32\pi G} \langle \partial_\mu h_{\alpha\beta} \partial_\nu h^{\alpha\beta} \rangle. \quad (4.7)$$

For a plane wave, using the TT gauge

$$t_{00} = \frac{c^2}{32\pi G} \langle \dot{h}_{ij}^{\text{TT}} \dot{h}_{ij}^{\text{TT}} \rangle = \frac{c^2}{16\pi G} \langle \dot{h}_+^2 + \dot{h}_\times^2 \rangle, \quad (4.8)$$

and the GW energy flux per unit area is

$$\frac{dE}{dt dA} = \frac{c^3}{16\pi G} \langle \dot{h}_+^2 + \dot{h}_\times^2 \rangle. \quad (4.9)$$

For a supernovae  $dE/(dt dA) \sim c^3 f^2 h^2 / (16\pi G) \sim 400 \text{erg}/(\text{cm}^2 \text{sec})$ , where we set  $h = 10^{-21}$  and  $f = 1 \text{ kHz}$ . The GW burst has a duration of a few msec. It is telling to compare it with the neutrino energy flux  $\sim 10^5 \text{erg}/(\text{cm}^2 \text{sec})$  and the photon energy flux (optical radiation)  $\sim 10^{-4} \text{erg}/(\text{cm}^2 \text{sec})$  from a supernovae. Neutrinos and optical radiation are emitted during a few seconds and one week, respectively.

## 5. Generation of gravitational waves

### 5.1. Sources in slow motion, weak-field and negligible self-gravity

In this section we evaluate the leading order contribution to the metric perturbations under the assumption that the internal motions of the source are slow compared to the speed of light. We also assume that the source's self-gravity is negligible. Henceforth, we shall discuss how to extend those results to sources with non-negligible self-gravity. We start from

$$\square \bar{h}_{\mu\nu} = -\frac{16\pi G}{c^4} T_{\mu\nu}, \quad \partial_\mu \bar{h}^{\mu\nu} = 0, \quad \partial_\mu T^{\mu\nu} = 0, \quad (5.1)$$

and introduce retarded Green functions

$$G(x - x') = -\frac{1}{4\pi} \frac{1}{|\mathbf{x} - \mathbf{x}'|} \delta\left(t - \frac{|\mathbf{x} - \mathbf{x}'|}{c} - t'\right), \quad (5.2)$$

which satisfy  $\square_x G(x - x') = \delta^{(4)}(x - x')$ . The solution of Eq. (5.1) can be written as

$$\bar{h}_{\mu\nu}(x) = -\frac{16\pi G}{c^4} \int d^4 x' G(x - x') T_{\mu\nu}(x'). \quad (5.3)$$

Outside the source, using the TT gauge, we have

$$\bar{h}_{ij}^{\text{TT}}(t, \mathbf{x}) = \Lambda_{ij,kl}(\mathbf{n}) \frac{4G}{c^4} \int d^3 x' \frac{1}{|\mathbf{x} - \mathbf{x}'|} T_{kl} \left( t - \frac{|\mathbf{x} - \mathbf{x}'|}{c}; \mathbf{x}' \right). \quad (5.4)$$

Denoting by  $d$  the typical size of the source, assuming to be far from the source, i.e.  $r \gg d$ , we can write  $|\mathbf{x} - \mathbf{x}'| = r - \mathbf{x}' \cdot \mathbf{n} + \mathcal{O}(d^2/r)$ , and Eq. (5.3) becomes

$$\bar{h}_{ij}^{\text{TT}}(t, \mathbf{x}) \simeq \frac{1}{r} \frac{4G}{c^4} \Lambda_{ij,kl}(\mathbf{n}) \int_{|\mathbf{x}'| < d} d^3 x' T_{kl} \left( t - \frac{r}{c} + \frac{\mathbf{x}' \cdot \mathbf{n}}{c}; \mathbf{x}' \right). \quad (5.5)$$

We can simplify the above equations if we assume that typical velocities inside the sources are much smaller than the speed of light  $c$ . If  $\omega$  is the typical frequency associated to the source motion, typical source velocities are  $v \sim \omega d$ . As we shall see in the following, the GW signal is determined by the leading multipole moments, thus  $\omega_{\text{GW}} \sim \omega \sim v/d$  and  $\lambda_{\text{GW}} \sim (c/v) d$ . If  $v/c \ll 1$ , we have  $\lambda_{\text{GW}} \gg d$ .

Applying a Fourier decomposition, we can write

$$T_{kl} \left( t - \frac{r}{c} + \frac{\mathbf{x}' \cdot \mathbf{n}}{c}; \mathbf{x}' \right) = \int \frac{d^4 k}{(2\pi)^4} \tilde{T}_{kl}(\omega, \mathbf{k}) \times e^{-i\omega \left( t - \frac{r}{c} + \frac{\mathbf{x}' \cdot \mathbf{n}}{c} \right) + i\mathbf{k} \cdot \mathbf{x}'}, \quad (5.6)$$

using  $\omega \mathbf{x}' \cdot \mathbf{n} \sim \omega d/c \ll 1$ , expanding the exponential and Taylor-expanding  $T_{kl}$  we get

$$\begin{aligned} h_{ij}^{\text{TT}}(t, \mathbf{x}) \simeq & \frac{1}{r} \frac{4G}{c^4} \Lambda_{ij,kl}(\mathbf{n}) \left[ \int d^3 x T^{kl}(t, \mathbf{x}) + \right. \\ & \frac{1}{c} n_m \frac{d}{dt} \int d^3 x T^{kl}(t, \mathbf{x}) x^m + \\ & \left. \frac{1}{2c^2} n_m n_p \frac{d^2}{dt^2} \int d^3 x T^{kl}(t, \mathbf{x}) x^m x^p + \dots \right]_{|t-r/c}. \quad (5.7) \end{aligned}$$

The above expression is valid in linearized gravity and for negligible self-gravity sources, i.e. for sources whose dynamics is not determined by gravitational forces. We notice that in Eq. (5.7) the higher multipoles are suppressed by a factor  $v/c$ . To make Eq. (5.7) more transparent, we can express the momenta  $T^{ij}$

in terms of the momenta of  $T^{00}$  and  $T^{0i}$ . Let us first introduce the momenta of the mass density

$$M = \frac{1}{c^2} \int d^3x T^{00}(t, \mathbf{x}), \quad (5.8)$$

$$M^i = \frac{1}{c^2} \int d^3x T^{00}(t, \mathbf{x}) x^i, \quad (5.9)$$

$$M^{ij} = \frac{1}{c^2} \int d^3x T^{00}(t, \mathbf{x}) x^i x^j, \quad (5.10)$$

$$(5.11)$$

and impose the conservation law  $\partial_\mu T^{\mu\nu} = 0$  valid in linearized gravity. Setting  $\nu = 0$ , we have  $\partial_0 T^{00} + \partial_i T^{i0} = 0$ , integrating this equation in a volume containing the source, we obtain the conservation of the mass  $\dot{M} = 0$ . Similarly, one can prove the conservation of the momentum  $\dot{M}^i = 0$ . Moreover, we have

$$\begin{aligned} c \dot{M}^{ij} &= \int_V d^3x x^i x^j \partial_0 T^{00} = - \int_V d^3x x^i x^j \partial_k T^{0k} \\ &= \int_V d^3x (x^j T^{0i} + x^i T^{0j}), \end{aligned} \quad (5.12)$$

where the second line is obtained after integrating by parts. Finally,

$$\ddot{M}^{ij} = 2 \int_V d^3x T^{ij}. \quad (5.13)$$

Thus, the leading term in Eq. (5.7), can be rewritten as

$$h_{ij}^{\text{TT}}(t, \mathbf{x}) = \frac{1}{r} \frac{2G}{c^4} \Lambda_{ij,kl}(\mathbf{n}) \ddot{M}^{kl} \left( t - \frac{r}{c} \right), \quad (5.14)$$

where  $M^{kl}$  is given by Eq. (5.11). The quantity  $T^{00}/c^2$  in Eq. (5.11) is a mass density. Besides the rest-mass contribution, it can contain terms due to the kinetic energy and the potential energy. For sources having strong gravitational field, as NSs and BHs, the mass density can depend also on the binding energy. Only for weak fields and small velocities, which is the assumption so far made,  $T^{00}/c^2$  reduces to the rest-mass density  $\rho$ .

Henceforth, we shall discuss some applications to binary systems and pulsars, so it is convenient to compute explicitly  $h_+$  and  $h_\times$ . Assuming that the GW propagates along the direction  $\mathbf{n} = (\cos \phi \sin \theta, \sin \phi \sin \theta, \cos \theta)$ , a straight

calculations gives:

$$h_+ = \frac{G}{r c^4} \left\{ \ddot{M}_{11} (\sin^2 \phi - \cos^2 \theta \cos^2 \phi) + \ddot{M}_{22} (\cos^2 \phi - \cos^2 \theta \sin^2 \phi) - \ddot{M}_{33} \sin^2 \theta - \ddot{M}_{12} \sin 2\phi (1 + \cos^2 \theta) + \ddot{M}_{13} \cos \phi \sin 2\theta + \ddot{M}_{23} \sin 2\theta \sin \phi \right\}, \quad (5.15)$$

$$h_\times = \frac{2G}{r c^4} \left\{ \frac{1}{2} (\ddot{M}_{11} - \ddot{M}_{22}) \cos \theta \sin 2\phi - \ddot{M}_{12} \cos \theta \cos 2\phi - \ddot{M}_{13} \sin \theta \sin \phi + \ddot{M}_{23} \cos \phi \sin \theta \right\}. \quad (5.16)$$

### 5.2. Sources in slow motion and weak-field, but non-negligible self-gravity

As already stated above, the derivation in linearized gravity of the quadrupole formula (5.14) cannot be applied to systems like binary stars whose dynamics is dominated by gravitational forces. In fact, because of the conservation-law valid in linearized gravity  $\partial_\mu T_{\mu\nu} = 0$ , the two bodies move along geodesics in Minkowski spacetime. The extension to the case in which self-gravity is non-negligible can be done as follows [47].

In full general relativity one can define the field  $H_{\mu\nu}$  such that

$$\sqrt{-g} g^{\mu\nu} = \eta^{\mu\nu} - H^{\mu\nu}, \quad (5.17)$$

where in the weak-field limit  $H^{\mu\nu}$  coincides with the reverse-trace tensor that we introduced above. Imposing the harmonic gauge  $\partial_\mu H^{\mu\nu} = 0$ , one derives

$$\square H_{\mu\nu} = -\frac{16\pi G}{c^4} [(-g) T_{\mu\nu} + \tau_{\mu\nu}], \quad (5.18)$$

where  $\tau_{\mu\nu}$  is the pseudotensor depending on  $H_{\mu\nu}$  that can be read explicitly from Refs. [14, 29]. The conservation law reads in this case

$$\partial_\mu [(-g) T^{\mu\nu} + \tau^{\mu\nu}] = 0. \quad (5.19)$$

We can redo the derivation in linearized gravity (see Sec. 2.2), but replace  $T_{\mu\nu} \rightarrow (-g) T_{\mu\nu} + \tau_{\mu\nu}$ , obtaining for the leading term in Eq. (5.14)  $\int T_{00} x^i x^j d^3x \rightarrow \int (T_{00} + \tau_{00}) x^i x^j d^3x$ . For sources characterized by weak gravity  $\tau_{00}$  is negligible with respect to  $T_{00}$ . Even though at the end one obtains the same formula, it is crucial to take into account the second order corrections in  $h_{\mu\nu}$ , i.e. the field  $\tau_{\mu\nu}$ , in the conservation law. Otherwise the sources would be obliged to move along geodesics in Minkowski spacetime, instead of moving in a bounded orbit.

### 5.3. Radiated energy, angular momentum and linear momentum

Using the results of Sec. 4, we can compute the power radiated at leading order

$$\frac{dP}{d\Omega} = \frac{r^2 c^3}{32\pi G} \langle \dot{h}_{ij}^{\text{TT}} \dot{h}_{ij}^{\text{TT}} \rangle = \frac{G}{8\pi c^5} \Lambda_{kl,mp}(\mathbf{n}) \langle \ddot{Q}_{kl} \ddot{Q}_{mp} \rangle, \quad (5.20)$$

where we introduce the traceless quadrupole tensor

$$Q_{ij} = M_{ij} - \frac{1}{3} \delta_{ij} M_{kk}. \quad (5.21)$$

Using the following relations

$$\int \frac{d\Omega}{4\pi} n_i n_j = \frac{1}{3} \delta_{ij}, \quad (5.22)$$

$$\int \frac{d\Omega}{4\pi} n_i n_j n_k n_l = \frac{1}{15} (\delta_{ij} \delta_{kl} + \delta_{ik} \delta_{jl} + \delta_{il} \delta_{jk}), \quad (5.23)$$

we derive for the total power radiated

$$P = \frac{G}{5c^5} \langle \ddot{Q}_{ij} \ddot{Q}_{ij} \rangle. \quad (5.24)$$

In the literature Eq. (5.24) is generally denoted as the *quadrupole formula*.

GWs not only carry away from the source the energy, but also angular momentum and linear momentum. At leading-order the angular-momentum radiated is [35]

$$\frac{dL^i}{dt} = \frac{2G}{5c^5} \epsilon^{ijk} \langle \ddot{Q}_{jl} \ddot{Q}_{lk} \rangle \quad (5.25)$$

while the linear momentum radiated is given by [35]

$$\frac{dP^i}{dt} = -\frac{G}{8\pi c^5} \int d\omega \ddot{Q}_{jk}^{\text{TT}} \partial^i \ddot{Q}_{jk}^{\text{TT}}. \quad (5.26)$$

Under parity,  $\mathbf{x} \rightarrow -\mathbf{x}$ , the mass quadrupole does not vary, and the integral in Eq. (5.26) is overall odd and vanishes. The first nonzero contribution comes at order  $\mathcal{O}(1/c^7)$  from the interference between the mass quadrupole and the sum of the octupole and current quadrupole. As a consequence of the loss of linear momentum through GW emission, the BH formed by the coalescence of a BH binary can acquire a kick or recoil velocity. The recoil velocity is astrophysically significant. If it were too large, the BH can be ejected from the host galaxy with important consequences on BH's mass growth through hierarchical mergers. Recently, there have been a plethora of numerical [48] and analytic [49] predictions.

The above discussion on energy, angular momentum and linear-momentum can be made more rigorous and applicable to sources with non-negligible self gravity thanks to the work of Bondi in the 50s [50]. Let us consider a sphere  $\mathcal{S}$  of volume  $\mathcal{V}$  and radius  $r$  containing the source. Be  $r$  much larger than the source dimension and the gravitational wavelength (far zone). It can be proven [29, 50] that  $P^\mu$ , defined by<sup>2</sup>

$$P^\mu = \int \tau^{\mu 0} d^3x, \quad (5.27)$$

is a four vector with respect to Lorentz transformations. Using the relation  $\partial_\mu \tau^{\mu\nu} = 0$ , we can write

$$\frac{dP^\mu}{dt} = \int_{\mathcal{V}} \partial_0 \tau^{\mu 0} d^3x = - \oint_{\mathcal{S}} \tau^{\mu i} n^i dS. \quad (5.28)$$

For  $\mu = 0$  the above equation gives the conservation of the energy

$$\frac{dP^0}{dt} = -r^2 \oint d\Omega \tau^{0i} n_i, \quad (5.29)$$

for  $\mu = j$  Eq. (5.28) gives the conservation of the linear momentum

$$\frac{dP^j}{dt} = -r^2 \oint d\Omega \tau^{ji} n_i. \quad (5.30)$$

## 6. Application to binary systems

### 6.1. Inspiral waveforms at leading Newtonian order

Let us consider a binary system with masses  $m_1$  and  $m_2$ , total mass  $M = m_1 + m_2$ , reduced mass  $\mu = m_1 m_2 / (m_1 + m_2)$  and symmetric mass-ratio  $\nu = \mu / M$ . We first assume that the two bodies are rather separated and move along a circular orbit. In the center-of-mass frame we can write for the relative coordinates

$$X(t) = R \cos \omega t, \quad Y(t) = R \sin \omega t, \quad Z(t) = 0, \quad (6.1)$$

$R$  being the relative distance between the two bodies. The only nonzero components of the tensor  $M^{ij} = \mu X^i X^j$  are

$$M_{11} = \frac{1}{2} \mu R^2 (1 + \cos 2\omega t), \quad (6.2)$$

$$M_{22} = \frac{1}{2} \mu R^2 (1 - \cos 2\omega t), \quad (6.3)$$

$$M_{12} = \frac{1}{2} \mu R^2 \sin 2\omega t. \quad (6.4)$$

---

<sup>2</sup>Note that the integration is done over a constant-time hypersurface.

Taking time-derivatives and plugging the above expressions in Eqs. (5.14), (5.15) we obtain

$$h_+(t) = \frac{1}{r} \frac{4G}{c^4} \mu R^2 \omega^2 \frac{(1 + \cos^2 \theta)}{2} \cos(2\omega t), \quad (6.5)$$

$$h_\times(t) = \frac{1}{r} \frac{4G}{c^4} \mu R^2 \omega^2 \cos \theta \sin(2\omega t), \quad (6.6)$$

where we shift the origin of time to get rid of the dependence on  $\phi$  and trade the retarded time with  $t$ .

For  $\theta = 0$ , i.e. along the direction perpendicular to the orbital plane,  $h_+$  and  $h_\times$  are both different from zero, and  $h_\times \pm i h_+ \propto \pm i e^{-2i\omega t}$ , thus the wave is circularly polarized. For  $\theta = \pi/2$ , i.e. along the orbital plane, only  $h_+$  is different from zero and the wave is linearly polarized.

The angular distribution of the radiated power is given by Eq. (5.24). It reads

$$\left( \frac{dP}{d\Omega} \right) = \frac{2G \mu^2 R^4 \omega^6}{\pi c^5} \mathcal{P}(\theta), \quad (6.7)$$

$$\mathcal{P}(\theta) = \frac{1}{4} (1 + 6 \cos^2 \theta + \cos^4 \theta). \quad (6.8)$$

The maximum power is emitted along the direction perpendicular to the orbital plane,  $\theta = 0$ , where  $\mathcal{P}(\pi/2) = 2$ . Since in the case of a binary system, there is always a component of the source's motion perpendicular to the observation direction, the power radiated does not vanish in any direction. Integrating over the total solid angle, we obtain the total power radiated,

$$P = \frac{32}{5} \frac{G \mu^2 R^4 \omega^6}{c^5}. \quad (6.9)$$

If we consider the binary system composed of Jupiter and the Sun, using  $m_J = 1.9 \times 10^{30}$  g,  $R = 7.8 \times 10^{13}$  cm and  $\omega = 1.68 \times 10^{-7}$  Hz, we get  $P = 5 \times 10^3$  Joules/sec. This value is tiny, especially when compared to the luminosity of the Sun in electromagnetic radiation  $P_\odot = 3.9 \times 10^{26}$  Joules/sec. If the binary moves along an eccentric orbit the power radiated is [51]

$$P = \frac{32}{5} \frac{G^4 \mu^2 M^2}{a^5 c^5} \frac{1}{(1 - e^2)^{7/2}} \left( 1 + \frac{73}{24} e^2 + \frac{37}{96} e^4 \right), \quad (6.10)$$

where  $a$  is the semi-major axis and  $e$  the eccentricity. Plugging in Eq. (6.10) the values for the Hulse-Taylor binary pulsar [52],  $a = 1.95 \times 10^{11}$  cm,  $m_1 = 1.441 M_\odot$ ,  $m_2 = 1.383 M_\odot$ ,  $e = 0.617$ , we get that the power radiated is  $7.35 \times 10^{24}$  Joules/sec, which is about 2% of the luminosity of the Sun in electromagnetic radiation.



The emission of GWs costs energy and to compensate for the loss of energy, the radial separation  $R$  between the two bodies must decrease. We shall now derive how the orbital frequency and GW frequency change in time, using Newtonian dynamics and the balance equation

$$\frac{dE_{\text{orbit}}}{dt} = -P. \quad (6.11)$$

At Newtonian order,  $E_{\text{orbit}} = -G m_1 m_2 / (2R)$  and  $\omega^2 = G M / R^3$ . Thus,  $\dot{R} = -2/3 (R\omega) (\dot{\omega}/\omega^2)$ . As long as  $\dot{\omega}/\omega^2 \ll 1$ , the radial velocity is smaller than the tangential velocity and the binary's motion is well approximated by an adiabatic sequence of quasi-circular orbits. Equation (6.11) implies that the orbital frequency varies as

$$\frac{\dot{\omega}}{\omega^2} = \frac{96}{5} \nu \left( \frac{GM\omega}{c^3} \right)^{5/3}, \quad (6.12)$$

and the GW frequency  $f_{\text{GW}} = 2\omega$ ,

$$\dot{f}_{\text{GW}} = \frac{96}{5} \pi^{8/3} \left( \frac{G\mathcal{M}}{c^3} \right)^{5/3} f_{\text{GW}}^{11/3}, \quad (6.13)$$

where  $\mathcal{M} = \mu^{3/5} M$  is the so-called *chirp* mass. Introducing the time to coalescence  $\tau = t_{\text{coal}} - t$ , and integrating Eq. (6.13), we get

$$f_{\text{GW}} \simeq 130 \left( \frac{1.21M_{\odot}}{\mathcal{M}} \right)^{5/8} \left( \frac{1\text{sec}}{\tau} \right)^{3/8} \text{ Hz}, \quad (6.14)$$

where  $1.21M_{\odot}$  is the chirp mass of a NS-NS binary. Equation (6.14) predicts coalescence times of  $\sim 17\text{min}$ ,  $2\text{sec}$ ,  $1\text{msec}$ , for  $f_{\text{GW}} \sim 10, 100, 10^3$  Hz. Using the above equations, it is straightforward to compute the relation between the radial separation and the GW frequency, we find

$$R \simeq 300 \left( \frac{M}{2.8M_{\odot}} \right)^{1/3} \left( \frac{100\text{ Hz}}{f_{\text{GW}}} \right)^{2/3} \text{ km}. \quad (6.15)$$

Finally, a useful quantity is the number of GW cycles, defined by

$$\mathcal{N}_{\text{GW}} = \frac{1}{\pi} \int_{t_{\text{in}}}^{t_{\text{fin}}} \omega(t) dt = \frac{1}{\pi} \int_{\omega_{\text{in}}}^{\omega_{\text{fin}}} \frac{\omega}{\dot{\omega}} d\omega. \quad (6.16)$$

Assuming  $\omega_{\text{fin}} \gg \omega_{\text{in}}$ , we get

$$\mathcal{N}_{\text{GW}} \simeq 10^4 \left( \frac{\mathcal{M}}{1.21M_{\odot}} \right)^{-5/3} \left( \frac{f_{\text{in}}}{10\text{Hz}} \right)^{-5/3}. \quad (6.17)$$

### 6.2. Inspiral waveform including post-Newtonian corrections

Already in the early developments of Einstein theory, an approximation method called post-Newtonian (PN) method was developed by Einstein, Droste and De Sitter. This method allowed theorists to draw quickly several observational consequences, and within one year of the discovery of general relativity, led to the predictions of the relativistic advance of the perihelion of planets, the gravitational redshift and the deflection of light.

The PN method involves an expansion around the Newtonian limit keeping terms of higher order in the small parameter [12, 14]

$$\epsilon \sim \frac{v^2}{c^2} \sim |h_{\mu\nu}| \sim \left| \frac{\partial_0 h}{\partial_i h} \right|^2 \sim \left| \frac{T^{0i}}{T^{00}} \right| \sim \left| \frac{T^{ij}}{T^{00}} \right|. \quad (6.18)$$

In order to be able to determine the dynamics of binary systems with a precision acceptable for detection, it has been necessary to compute the force determining the motion of the two bodies and the amplitude of the gravitational radiation with a precision going beyond the quadrupole formula (5.14). For nonspinning BHs, the two-body equations of motion and the GW flux are currently known through 3.5PN order [13]. If we restrict the discussion to circular orbits, as Eq. (6.12) shows, there exists a natural *adiabatic* parameter  $\dot{\omega}/\omega^2 = \mathcal{O}[(v/c)^5]$ . Higher-order PN corrections to Eq. (6.12) have been computed [13, 15], yielding ( $G = 1 = c$ )

$$\frac{\dot{\omega}}{\omega^2} = \frac{96}{5} \nu v_\omega^{5/3} \sum_{k=0}^7 \omega_{(k/2)\text{PN}} v_\omega^{k/3} \quad (6.19)$$

where we define  $v_\omega \equiv (M \omega)^{1/3}$  and

$$\omega_{0\text{PN}} = 1, \quad (6.20)$$

$$\omega_{0.5\text{PN}} = 0, \quad (6.21)$$

$$\omega_{1\text{PN}} = -\frac{743}{336} - \frac{11}{4} \nu, \quad (6.22)$$

$$\omega_{1.5\text{PN}} = 4\pi + \left[ -\frac{47}{3} \frac{S_\ell}{M^2} - \frac{25}{4} \frac{\delta m}{M} \frac{\Sigma_\ell}{M^2} \right], \quad (6.23)$$

$$\omega_{2\text{PN}} = \frac{34\,103}{18\,144} + \frac{13\,661}{2\,016} \nu + \frac{59}{18} \nu^2 - \frac{1}{48} \nu \chi_1 \chi_2 \left[ 247 (\hat{\mathbf{S}}_1 \cdot \hat{\mathbf{S}}_2) - 721 (\hat{\boldsymbol{\ell}} \cdot \hat{\mathbf{S}}_1) (\hat{\boldsymbol{\ell}} \cdot \hat{\mathbf{S}}_2) \right], \quad (6.24)$$

Table 1 Post-Newtonian contributions to the number of GW cycles accumulated from  $\omega_{\text{in}} = \pi \times 10$  Hz to  $\omega_{\text{fin}} = \omega^{\text{ISCO}} = 1/(6^{3/2} M)$  for binaries detectable by LIGO and VIRGO. We denote  $\kappa_i = \hat{\mathbf{S}}_i \cdot \hat{\boldsymbol{\ell}}$  and  $\xi = \hat{\mathbf{S}}_1 \cdot \hat{\mathbf{S}}_2$ .

	$(10 + 10)M_{\odot}$	$(1.4 + 1.4)M_{\odot}$
Newtonian	601	16034
1PN	+59.3	+441
1.5PN	$-51.4 + 16.0 \kappa_1 \chi_1 + 16.0 \kappa_2 \chi_2$	$-211 + 65.7 \kappa_1 \chi_1 + 65.7 \kappa_2 \chi_2$
2PN	$+4.1 - 3.3 \kappa_1 \kappa_2 \chi_1 \chi_2 + 1.1 \xi \chi_1 \chi_2$	$+9.9 - 8.0 \kappa_1 \kappa_2 \chi_1 \chi_2 + 2.8 \xi \chi_1 \chi_2$
2.5PN	$-7.1 + 5.5 \kappa_1 \chi_1 + 5.5 \kappa_2 \chi_2$	$-11.7 + 9.0 \kappa_1 \chi_1 + 9.0 \kappa_2 \chi_2$
3PN	+2.2	+2.6
3.5PN	-0.8	-0.9

$$\omega_{2.5\text{PN}} = -\frac{1}{672} (4159 + 15876\nu) \pi + \left[ \left( -\frac{31811}{1008} + \frac{5039}{84} \nu \right) \frac{S_{\ell}}{M^2} + \left( -\frac{473}{84} + \frac{1231}{56} \nu \right) \frac{\delta m \Sigma_{\ell}}{M M^2} \right], \quad (6.25)$$

$$\omega_{3\text{PN}} = \left( \frac{16447322263}{139708800} - \frac{1712}{105} \gamma_E + \frac{16}{3} \pi^2 \right) + \left( -\frac{56198689}{217728} + \frac{451}{48} \pi^2 \right) \nu + \frac{541}{896} \nu^2 - \frac{5605}{2592} \nu^3 - \frac{856}{105} \log[16\nu^2], \quad (6.26)$$

$$\omega_{3.5\text{PN}} = \left( -\frac{4415}{4032} + \frac{358675}{6048} \nu + \frac{91495}{1512} \nu^2 \right) \pi. \quad (6.27)$$

We denote  $\boldsymbol{\ell} = \mu \mathbf{X} \times \mathbf{V}$  the Newtonian angular momentum (with  $\mathbf{X}$  and  $\mathbf{V}$  the two-body center-of-mass radial separation and relative velocity), and  $\hat{\boldsymbol{\ell}} = \boldsymbol{\ell}/|\boldsymbol{\ell}|$ ;  $\mathbf{S}_1 = \chi_1 m_1^2 \hat{\mathbf{S}}_1$  and  $\mathbf{S}_2 = \chi_2 m_2^2 \hat{\mathbf{S}}_2$  are the spins of the two bodies (with  $\hat{\mathbf{S}}_{1,2}$  unit vectors, and  $0 < \chi_{1,2} < 1$  for BHs) and

$$\mathbf{S} \equiv \mathbf{S}_1 + \mathbf{S}_2, \quad \Sigma \equiv M \left[ \frac{\mathbf{S}_2}{m_2} - \frac{\mathbf{S}_1}{m_1} \right]. \quad (6.28)$$

Finally,  $\delta m = m_1 - m_2$  and  $\gamma_E = 0.577\dots$  is Euler's constant.

It is instructive to compute the relative contribution of the PN terms to the total number of GW cycles accumulating in the frequency band of LIGO/VIRGO. In Table 1, we list the figures obtained by plugging Eq. (6.19) into Eq. (6.16). As final frequency we use the innermost stable circular orbit (ISCO) of a point particle in Schwarzschild [ $f_{\text{GW}}^{\text{ISCO}} \simeq 4400/(M/M_{\odot})$  Hz].

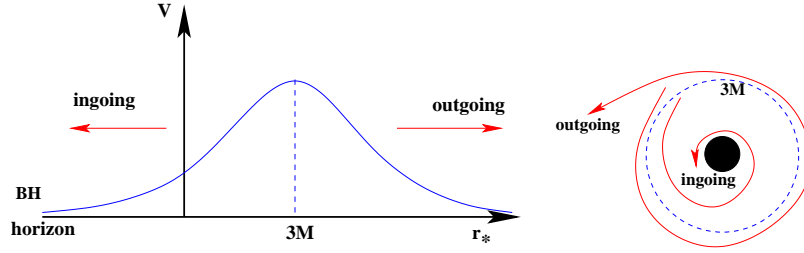


Fig. 4. We sketch the curvature potential as function of the tortoise coordinate  $r^*$  associated to metric perturbations of a Schwarzschild BH. The potential peaks at the last unstable orbit for a massless particle (the light ring). Ingoing modes propagate toward the BH horizon, whereas outgoing modes propagate away from the source.

### 6.3. Full waveform: inspiral, merger and ring-down

After the two BHs merge, the system settles down to a Kerr BH and emits quasinormal modes (QNMs), as originally predicted by Ref. [53, 54]. This phase is commonly known as the ring-down (RD) phase. Since the QNMs have complex frequencies totally determined by the BH's mass and spin, the RD waveform is a superposition of damped sinusoidals. The inspiral and RD waveforms can be computed analytically. What about the merger? Since the nonlinearities dominate, the merger would be described at *best* and *utterly* through numerical simulations of Einstein equations. However, before NR results became available, some analytic approaches were proposed. In the test-mass limit,  $\nu \ll 1$ , Refs. [54, 55] realized a long time ago that the basic physical reason underlying the presence of a universal merger signal was that when a test particle falls below  $3M$  (the unstable light storage ring of Schwarzschild), the GW it generates is strongly filtered by the curvature potential barrier centered around it (see Fig. 4). For the equal-mass case  $\nu = 1/4$ , Price and Pullin [56] proposed the so-called close-limit approximation, which consists in switching from the two-body description to the one-body description (perturbed-BH) close to the light-ring location. Based on these observations, the effective-one-body (EOB) resummation scheme [16] provided a first *example* of full waveform by (i) resumming the PN Hamiltonian, (ii) modeling the merger as a very short (instantaneous) phase and (iii) matching the end of the plunge (around the light-ring) with the RD phase (see Ref. [57] where similar ideas were developed also in NR). The matching was initially done using *only* the least damped QNM whose mass and spin were determined by the binary BH energy and angular momentum at the end of the plunge. An example of full waveform is given in Fig. 5. Today, with the spectacular results in NR, we are in the position of assessing the closeness of analytic to numerical waveforms for in-

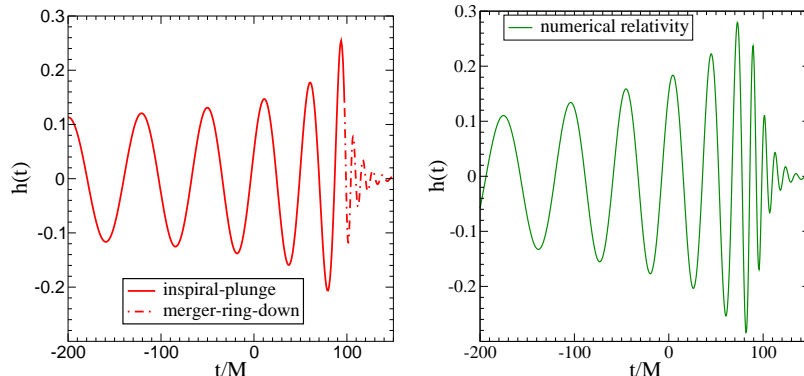


Fig. 5. On the left panel we show the GW signal from an equal-mass nonspinning BH binary as predicted at 2.5PN order by Buonanno and Damour (2000) in Ref. [16]. The merger is assumed almost instantaneous and one QNM is included. On the right panel we show the GW signal from an equal-mass BH binary with a small spin  $\chi_1 = \chi_2 = 0.06$  obtained in full general relativity by Pretorius [58]

spiral, merger and RD. In Fig. 6, we show some first-order comparisons between the EOB-analytic and NR waveforms [58] (see also Ref. [59]). Similar results for the inspiral phase but using PN theory [13, 15] (without resummation) at 3.5PN order are given in Refs. [58, 59]. So far, the agreement is qualitatively good, but more accurate simulations, starting with the BHs farther apart, are needed to draw robust conclusions.

Those comparisons are suggesting that it should be possible to design purely analytic templates with the full numerics used to guide the patching together of the inspiral and RD waveforms. This is an important avenue to template construction as eventually hundreds of thousands of waveform templates may be needed to extract the signal from the noise, an impossible demand for NR alone.

#### 6.4. Inspiral templates for data analysis

The search for GWs from coalescing binaries with laser interferometer GW detectors is based on the matched-filtering technique, which requires accurate knowledge of the waveform (or template) of the incoming signal. As an example, in this section we derive the inspiral GW template in Fourier domain using the stationary phase approximation (SPA). Those templates are currently used to search for inspiraling binary with LIGO/VIRGO/GEO/TAMA detectors. Henceforth, we use  $G = 1 = c$ .

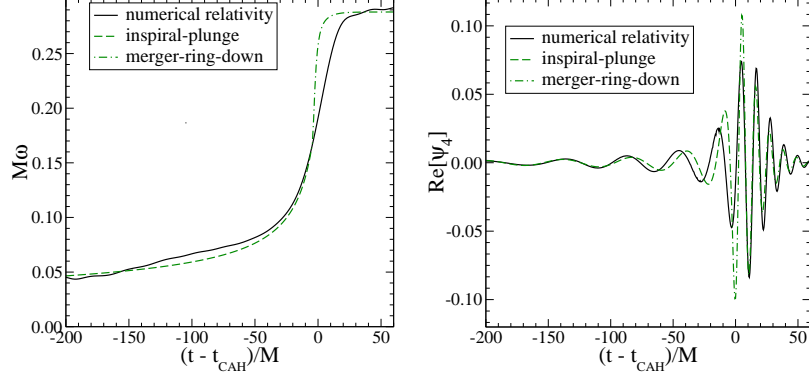


Fig. 6. Comparison between inspiral-merger-ring-down frequency (left panel) and waveform (right panel) for an equal-mass BH binary with spin  $\chi_1 = \chi_2 = 0.06$ , as predicted at 3.5PN order in Ref. [16] and as obtained in a numerical simulation by Pretorius [58]. In the analytic model the merger is assumed almost instantaneous and three QNMs are included [58].  $\Psi_4$  is the Weyl tensor proportional to the second derivative of  $h$ ; we denote with  $t_{\text{CAH}}$  the time when the apparent common horizon forms.

The detector response to a GW signal is given by [24]

$$h(t) = h_+(t) F_+ + h_\times(t) F_\times, \quad (6.29)$$

$$F_+ = \frac{1}{2}(1 + \cos^2 \Theta) \cos 2\Phi \cos 2\Psi - \cos \Theta \sin 2\Phi \sin 2\Psi, \quad (6.30)$$

$$F_\times = \frac{1}{2}(1 + \cos^2 \Theta) \cos 2\Phi \sin 2\Psi + \cos \Theta \sin 2\Phi \cos 2\Psi, \quad (6.31)$$

being  $\Theta, \Phi, \psi$  the angles defining the relative orientation of the binary with respect to the detector [24]. It is convenient to introduce the variables

$$\tilde{F}_+ \equiv \frac{(1 + \cos^2 \Theta) F_+}{[(1 + \cos^2 \Theta)^2 F_+^2 + 4 \cos^2 \Theta F_\times^2]^{1/2}}, \quad (6.32)$$

$$\tilde{F}_\times \equiv \frac{4 \cos^2 \Theta F_\times}{[(1 + \cos^2 \Theta)^2 F_+^2 + 4 \cos^2 \Theta F_\times^2]^{1/2}}. \quad (6.33)$$

Noticing that  $\tilde{F}_+^2 + \tilde{F}_\times^2 = 1$ , we can define  $\cos \xi \equiv \tilde{F}_+$  and  $\sin \xi \equiv \tilde{F}_\times$ , and

$$\mathcal{A}(\Theta, \Phi, \Psi; \theta) \equiv [(1 + \cos^2 \theta)^2 F_+^2 + 4 \cos^2 \theta F_\times^2]^{1/2}, \quad (6.34)$$

$$\tan \xi(\Theta, \Phi, \Psi; \theta) \equiv \frac{4 \cos^2 \theta F_\times}{(1 + \cos^2 \theta) F_+}. \quad (6.35)$$

The GW signal for an inspiraling binary (6.29) can be rewritten in the simpler form

$$h(t) = \frac{2\mathcal{M}}{r} \mathcal{A}(\Theta, \Phi, \Psi; \theta) [\mathcal{M}\omega(t)]^{2/3} \cos[2\phi(t) + 2\phi_0 - \xi]. \quad (6.36)$$

If we are not interested in recovering the binary's orientation with respect to the detector (the so-called *inverse* problem), we can absorb  $\xi$  into  $\phi_0$ , and average over the angles  $(\Theta, \Phi, \Psi, \theta)$  obtaining [24]  $\overline{\mathcal{A}^2} = 16/25$ .

Let us now compute the Fourier transform of the GW signal

$$\begin{aligned} \tilde{h}(f) &= \int_{-\infty}^{+\infty} e^{2\pi i f t} h(t) dt, \\ &= \frac{1}{2} \int_{-\infty}^{+\infty} dt A(t) \left[ e^{2\pi i f t + i\phi_{\text{GW}}(t)} + e^{2\pi i f t - i\phi_{\text{GW}}(t)} \right], \end{aligned} \quad (6.37)$$

where  $A(t) = (2\mathcal{M}/R) \sqrt{\mathcal{A}^2} [\mathcal{M}\omega(t)]^{2/3}$  and  $\phi_{\text{GW}}(t) = 2\phi(t) + 2\Phi_0$ . We compute the integral as follows. In Eq. (6.37) The dominant contribution comes from the vicinity of the *stationary* points in the phase. Assuming  $f > 0$ , we pose  $\psi(t) \equiv 2\pi f t - \phi_{\text{GW}}$  and impose  $(d\psi/dt)_{t_f} = 0$ , that is  $(d\phi_{\text{GW}}/dt)_{t_f} = 2\pi f = 2\pi F(t_f)$ . Expanding the phase up to quadratic order

$$\psi(t_f) = 2\pi f t_f - \phi_{\text{GW}}(t_f) - \pi \dot{F}(t_f) (t - t_f)^2, \quad (6.38)$$

we get

$$\tilde{h}_{\text{SPA}}(f) = \frac{1}{2} \frac{A(t_f)}{\sqrt{\dot{F}(t_f)}} e^{i[2\pi f t_f - \phi_{\text{GW}}(t_f)] - i\pi/4}. \quad (6.39)$$

To compute  $\phi_{\text{GW}}(t_f)$  and  $\dot{F}(t_f)$ , we need to solve the following equations

$$v^3 = \dot{\phi}_{\text{GW}} \frac{M}{2}, \quad \frac{dE}{dt}(v) = -\mathcal{F}(v), \quad (6.40)$$

where  $E$  is the center-of-mass energy and  $\mathcal{F}$  the GW energy flux. A direct calculation yields

$$t(v) = t_c + M \int_v^{v_c} dv \frac{E'(v)}{\mathcal{F}(v)}, \quad (6.41)$$

$$\phi_{\text{GW}}(v) = \phi_c + 2 \int_v^{v_c} dv v^3 \frac{E'(v)}{\mathcal{F}(v)}, \quad (6.42)$$

thus,

$$\psi(f) = 2\pi f t_c - \phi_c - \frac{\pi}{4} + 2 \int_v^{v_c} (v_c^3 - v^3) \frac{E'(v)}{\mathcal{F}(v)} dv, \quad (6.43)$$

Using Eq. (6.12), we have  $\dot{F}(t_f) \equiv \dot{\omega}/\pi = (96/5)(1/\pi)\nu M^{5/3}\omega^{11/3}$ , and we obtain [60]

$$\tilde{h}_{\text{SPA}}(f) = \mathcal{A}_{\text{SPA}}(f) e^{i\psi_{\text{SPA}}(f)}, \quad (6.44)$$

$$\mathcal{A}_{\text{SPA}}(f) = \frac{\sqrt{\mathcal{A}^2}}{r} \frac{1}{\pi^{2/3}} \left(\frac{5}{96}\right)^{1/2} \mathcal{M}^{5/6} f^{-7/6}, \quad (6.45)$$

$$\psi_{\text{SPA}}(f) = 2\pi f t_c - \phi_c - \frac{\pi}{4} + \frac{3}{128\nu v_f^5} \sum_{k=0}^7 \psi_{(k/2)\text{PN}} v_f^k, \quad (6.46)$$

where we denote  $v_f = (\pi M f)^{1/3}$ . The coefficients  $\psi_{(k/2)\text{PN}}$ 's,  $k = 0, \dots, 7$ , (with  $N = 7$  at 3.5PN order) in the Fourier phase are given by

$$\psi_{0\text{PN}} = 1, \quad (6.47a)$$

$$\psi_{0.5\text{PN}} = 0, \quad (6.47b)$$

$$\psi_{1\text{PN}} = \left(\frac{3715}{756} + \frac{55}{9}\nu\right), \quad (6.47c)$$

$$\psi_{1.5\text{PN}} = -16\pi + 4\beta, \quad (6.47d)$$

$$\psi_{2\text{PN}} = \left(\frac{15293365}{508032} + \frac{27145}{504}\nu + \frac{3085}{72}\nu^2\right) - 10\sigma, \quad (6.47e)$$

$$\psi_{2.5\text{PN}} = \pi \left(\frac{38645}{756} - \frac{65}{9}\nu\right) (1 + 3 \log v_f), \quad (6.47f)$$

$$\begin{aligned} \psi_{3\text{PN}} = & \left(\frac{11583231236531}{4694215680} - \frac{640\pi^2}{3} - \frac{6848\gamma_E}{21}\right) + \\ & \nu \left(-\frac{15737765635}{3048192} + \frac{2255\pi^2}{12}\right) + \\ & \frac{76055}{1728}\nu^2 - \frac{127825}{1296}\nu^3 - \frac{6848}{21}\log(4\nu), \end{aligned} \quad (6.47g)$$

$$\psi_{3.5\text{PN}} = \pi \left(\frac{77096675}{254016} + \frac{378515}{1512}\nu - \frac{74055}{756}\nu^2\right), \quad (6.47h)$$

where

$$\beta = \sum_{i=1}^2 \left(\frac{113}{12} \frac{m_i^2}{M^2} + \frac{25}{4}\nu\right) \chi_i \kappa_i, \quad (6.48)$$

$$\sigma = \nu \left(\frac{721}{48} \chi_1 \kappa_1 \chi_2 \kappa_2 - \frac{247}{48}\xi\right). \quad (6.49)$$



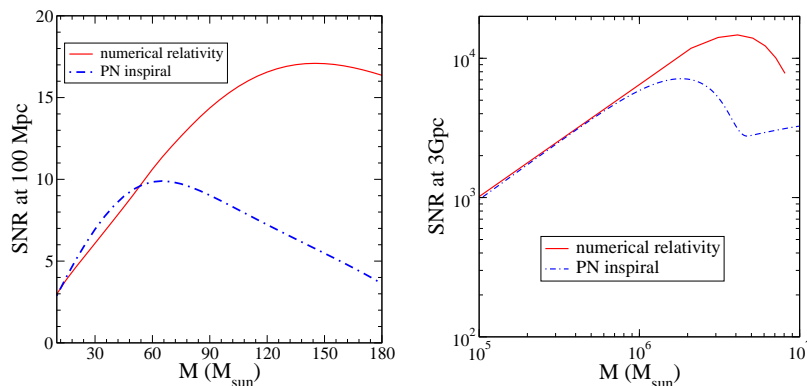


Fig. 7. We show the sky-averaged SNR for an equal-mass nonspinning binary when either the PN inspiral waveform (terminated at the PN ISCO) or the full NR waveform are included. The left panel uses the noise spectral density of LIGO, whereas the right panel the noise spectral density of LISA.

In alternative theories of gravity [61], such as Brans-Dicke theory or massive graviton theories, the SPA phase (6.46) contains the terms

$$\psi_{\text{SPA}}^{\text{alt th}}(f) = \frac{3}{128 \nu v_f^5} \left[ -\frac{5\mathcal{S}^2}{84\omega_{\text{BD}}} v_f^{-2} - \frac{128 \pi^2 D \nu M}{3 \lambda_g^2 (1+z)} v_f^2 \right]. \quad (6.50)$$

The first term in the square brace is the contribution of dipole gravitational radiation in Brans-Dicke theory. The scalar charge of the  $i$ -th body is  $\alpha_i = \bar{\alpha}\hat{\alpha}_i = \bar{\alpha}(1-2s_i)$ , where  $\bar{\alpha}^2 = 1/(2\omega_{\text{BD}}+3) \sim (2\omega_{\text{BD}})^{-1}$  in the limit  $\omega_{\text{BD}} \gg 1$ , and  $s_i$  is called the *sensitivity* of the  $i$ -th body (a measure of the self-gravitational binding energy per unit mass). The coefficient in the dipole term is  $\mathcal{S} = (\hat{\alpha}_1 - \hat{\alpha}_2)/2$ . The fact that it is dipole radiation means that it is proportional to  $v^{-2}$  compared to the quadrupole term, but the small size of  $\mathcal{S}$  and the large current solar-system bound on  $\omega_{\text{BD}} > 40,000$  make this a small correction. The second term in the square brace of Eq. (6.50) is the effect of a massive graviton, which alters the arrival time of waves of a given frequency, depending on the size of the graviton Compton wavelength  $\lambda_g$  and on a distance quantity  $D$ , defined in Ref. [62]. It is possible to put interesting bounds on  $\omega_{\text{BD}}$  and  $\lambda_g$  using LISA [61, 62].

Finally, the sky-average signal-to-noise ratio (SNR) for SPA waveforms is

$$\sqrt{\left(\frac{\mathcal{S}}{N}\right)^2} = \frac{1}{r} \frac{1}{\pi^{2/3}} \sqrt{\frac{2}{15}} \mathcal{M}^{5/6} \left[ \int_0^{f_{\text{fin}}} \frac{f^{-7/3}}{S_n(f)} \right]^{1/2}. \quad (6.51)$$

In the left panel of Fig. 7, we show the sky average SNRs versus total mass, for an equal-mass nonspinning binary at 100 Mpc using the noise-spectral density of

LIGO. Astrophysical observations and theoretical predictions suggest that stellar mass BHs have a total mass ranging between  $6\text{--}30M_\odot$ . If binary BHs of larger total mass exist, they could be detected by LIGO with high SNR. In the right panel of Fig. 7 we show the average SNR for one Michelson LISA configuration versus the total (redshifted) mass for an equal-mass nonspinning binary at 3 Gpc. The dip in the plot is due to the white-dwarf binary confusion noise. Due to the inclusion of merger and ring-down phases, the SNR increases considerably for total masses larger than  $2 \times 10^6 M_\odot$ .

## 7. Other astrophysical sources

### 7.1. Pulsars

The production of GWs from a rotating body is of considerable importance, in particular for application to isolated pulsars. For simplicity we shall examine the case the rigid body rotates around one of its principal axis.

Let us denote by  $(X'_1, X'_2, X'_3)$  the coordinates in the reference frame attached to the body, the so-called *body frame*, and introduce a *fixed frame* with coordinates  $(X_1, X_2, X_3)$ , oriented such that  $X'_3 = X_3$ . In both frames the origin of the axes coincides with the center-of-mass of the body. The two frames are related by the time-dependent rotation matrix

$$\mathcal{R}_{ij} = \begin{pmatrix} \cos \omega t & \sin \omega t & 0 \\ -\sin \omega t & \cos \omega t & 0 \\ 0 & 0 & 1 \end{pmatrix}, \quad (7.1)$$

where  $\omega$  is the rotation frequency. The inertia tensor of a rigid body is defined by

$$I^{ij} = \int d^3 X \rho(\mathbf{X}) (R^2 \delta^{ij} - X^i X^j), \quad (7.2)$$

$\rho$  being the mass density. Since any hermitian matrix can be diagonalized, there exists an orthogonal frame where  $I_{ij}$  is diagonal. The eigenvalues are called principal moments of inertia. The frame where the inertia tensor is diagonal is the body frame. We denote by  $I'_{ij} = \text{diag}(I_1, I_2, I_3)$  the inertia tensor in the  $(X'_1, X'_2, X'_3)$  coordinate system, and by  $I_{ij}$  its components in the  $(X_1, X_2, X_3)$  frame. Using the relation  $I = \mathcal{R}^t I' \mathcal{R}$ , it is straightforward to derive

$$I_{11} = 1 + \frac{1}{2} (I_1 - I_2) \cos(2\omega t), \quad (7.3)$$

$$I_{12} = \frac{1}{2} (I_1 - I_2) \sin(2\omega t), \quad (7.4)$$

$$I_{22} = 1 - \frac{1}{2}(I_1 - I_2) \cos(2\omega t), \quad (7.5)$$

$$I_{33} = I_3, \quad (7.6)$$

$$I_{13} = I_{23} = 0. \quad (7.7)$$

To get the leading-order GW signal, we need to compute the second-time derivative of the quadrupole tensor  $M_{ij} = \int d^3X \rho(\mathbf{X}) X^i X^j$ , i.e.  $\ddot{M}_{ij} = -\ddot{I}_{ij}$ . We obtain

$$M_{11} = -\frac{1}{2}(I_1 - I_2) \cos(2\omega t), \quad (7.8)$$

$$M_{12} = -\frac{1}{2}(I_1 - I_2) \sin(2\omega t), \quad (7.9)$$

$$M_{22} = \frac{1}{2}(I_1 - I_2) \cos(2\omega t). \quad (7.10)$$

Thus, if the body rotates around the principal axis  $X'_3$ , there is a time-varying second mass moment only if  $I_1 \neq I_2$ . Plugging in Eqs. (5.14), (5.15) the above expressions, yields

$$h_+ = \frac{1}{r} \frac{4G\omega^2}{c^4} (I_1 - I_2) \frac{(1 + \cos\theta)}{2} \cos(2\omega t), \quad (7.11)$$

$$h_\times = \frac{1}{r} \frac{4G\omega^2}{c^4} (I_1 - I_2) \cos\theta \sin(2\omega t). \quad (7.12)$$

The GW signal is emitted at twice the pulsar rotation frequency. It is common to define the ellipticity  $\epsilon = (I_1 - I_2)/I_3$  and  $h_0 = (4\pi^2 G/c^4)(I_3 f_{\text{GW}}^2/r)\epsilon$ . The value of the ellipticity depends on the NS properties, in particular the maximum strain that can be supported by its crust. Pulsars are thought to form in supernova explosions. The outer layers of the star crystallize as the newborn pulsar cools by neutrino emission. Anisotropic stresses during this phase could lead to values  $\epsilon \lesssim 10^{-6}$  [39], although with exotic equation of state  $\epsilon \simeq 10^{-5}$ – $10^{-4}$  [63]. Plugging numbers we find

$$h_0 \simeq 10^{-25} \left( \frac{\epsilon}{10^{-6}} \right) \left( \frac{I_3}{10^{45} \text{ g cm}^2} \right) \left( \frac{10 \text{ kpc}}{r} \right) \left( \frac{f_{\text{GW}}}{1 \text{ kHz}} \right)^2. \quad (7.13)$$

Using Eq. (5.24), we can compute the total power radiated

$$P = \frac{32}{5} \frac{G}{c^5} \epsilon^3 I_3^2 \omega^6. \quad (7.14)$$

Due to GW emission, the rotational energy of the star decreases as

$$\frac{dE}{dt} = -\frac{32}{5} \frac{G}{c^5} \epsilon^3 I_3^2 \omega^6. \quad (7.15)$$

Since the rotational energy of a star rotating around its principal axis is

$$E = \frac{1}{2} I_3 \omega^2, \quad (7.16)$$

if the GW emission were the dominant mechanism for the loss of rotational energy, the pulsar frequency should decrease as

$$\dot{\omega} = -\frac{32}{5} \frac{G}{c^5} \epsilon^2 I_3 \omega^5. \quad (7.17)$$

From electromagnetic observations one finds instead  $\dot{\omega} \propto -\omega^n$ , where  $n \simeq 2-3$ . Thus, the GW emission is not the major mechanism of energy loss for a rotating pulsar.

If the rotation axis does not coincide with a principal axis, the pulsar motion is a combination of rotation around the principal axis and precession. New features appear in the GW signal, as discussed in detail in Ref. [64].

The detection of continuous, monochromatic frequency waves is achieved by constructing power spectrum estimators and searching for statistically significant peaks at fixed frequencies for very long time. If  $T$  is the observation time, the signal-to-noise ratio grows like  $\sqrt{T}$ . The detection is complicated by the fact that the signal received at the detector is not perfectly monochromatic due to the Earth's motion. Because of Doppler shifts in frequency, the spectral lines of fixed frequency sources spread power into many Fourier bins about the observed frequency. Given the possibility that the strongest sources of continuous GWs may be electromagnetically invisible or previously undiscovered, an all sky, all frequency search for such unknown sources is very important, though computationally very expensive [25].

## 7.2. Supernovae

Supernovae are triggered by the violent collapse of a stellar core which forms a NS or BH. The core collapse proceeds extremely fast, lasting less than a second and the dense fluid undergoes motions with relativistic speeds. Small deviations from spherical symmetry during this phase can generate GWs.

From electromagnetic observations we know that stars with mass  $M > 8M_\odot$  end their evolution in core collapse and that 90% of them have mass between  $8-20M_\odot$ . During the collapse most of the material is ejected and if the progenitor star has a mass  $M \leq 20M_\odot$ , it leaves behind a NS. If  $M \geq 20M_\odot$ , more than 10% of the material falls back and pushes the proto-NS above the maximum NS mass, leading to a BH. If the progenitor star has a mass  $M \geq 40M_\odot$ , no supernovae takes place, the star collapses directly to a BH. Numerical simulations [65]

have predicted strains on the order of

$$h = 6 \times 10^{-17} \sqrt{\eta_{\text{eff}}} \left(\frac{M}{M_{\odot}}\right)^{1/2} \left(\frac{10\text{kpc}}{r}\right)^{1/2} \left(\frac{1\text{kHz}}{f}\right) \left(\frac{10\text{msec}}{\tau_{\text{collapse}}}\right)^{1/2}, \quad (7.18)$$

where  $\Delta E_{\text{GW}} = \eta_{\text{eff}} M c^2$ ,  $\eta_{\text{eff}} \sim 10^{-9}$ . Reference [65] pointed out that GWs could also be produced by neutrino emission during the supernovae explosion. The GW signal would extend toward lower frequencies  $\sim 10$  Hz. Moreover, the superposition of independent GW signals from cosmological supernovae may give rise to a stochastic GW background. While the estimates remain uncertain within several orders of magnitude, this background may become detectable by second-generation space-based interferometers operating around  $\sim 0.1$  Hz [66].

Note that after a supernovae explosion or a collapsar a significant amount of the ejected material can fall back, subsequently spinning and heating the NS or BH. Quasi-normal modes can be excited. There is also the possibility that the collapsed material might fragment into clumps which orbit for some cycles like a binary system or form bar-like structures, which also produced GW signals [67].

## 8. Cosmological sources

In this section we want to review stochastic GW backgrounds. Depending on its origin, the stochastic background can be broadly divided into two classes: the astrophysically generated background due to the incoherent superposition of gravitational radiation emitted by large populations of astrophysical sources that cannot be resolved individually [68], and the primordial GW background generated by processes taking place in the early stages of the Universe. A primordial component of such background is especially interesting, since it would carry unique information about the state of the primordial Universe.

The energy and spectral content of such radiation is encoded in the spectrum, defined as follows

$$\Omega_{\text{GW}} = \frac{1}{\rho_c} f \tilde{\rho}_{\text{GW}}(f), \quad (8.1)$$

where  $f$  is the frequency,  $\rho_c$  is the critical energy density of the Universe ( $\rho_c = 3H_0^2/8\pi G$ ) and  $\tilde{\rho}_{\text{GW}}$  is the GWs energy density per unit frequency, i.e.

$$\rho_{\text{GW}} = \int_0^{\infty} df \tilde{\rho}_{\text{GW}}(f). \quad (8.2)$$

Before discussing the mechanisms that might have generated a primordial GW background, we review the main phenomenological bounds.

### 8.1. Phenomenological bounds

The theory of big-bang nucleosynthesis (BBN) predicts rather successfully the primordial abundances of light elements. If at  $t_{\text{BBN}}$ , the contribution of primordial GWs (or any other extra energy component) to the total energy density were too large, then the expansion rate of the Universe  $H$  will be too large and the freeze-out temperature which determines the relative abundance of neutrons and protons will be too high. As a consequence, neutrons will be more available and light elements will be overproduced spoiling BBN predictions. Detailed calculations provide the following bound on the energy density [69]

$$\int d \ln f h_0^2 \Omega_{\text{GW}}(f) \leq 5.6 \times 10^{-6} (N_\nu - 3), \quad (8.3)$$

where  $N_\nu$  is the *effective number of neutrino species* at  $t_{\text{BBN}}$  [38]. The above bound extends to frequency (today) greater than  $\sim 10^{-10}$  Hz. More recently, Ref. [70] derived a similar bound by constraining the primordial GW energy density at the time of decoupling  $t_{\text{dec}}$ . The latter bound extends to lower frequency (today)  $\sim 10^{-15}$  Hz, being determined by the comoving horizon size at the time of decoupling.

Another important bound is the so-called COBE bound, which comes from the measurement of temperature fluctuations in the CMB produced by the Sachs-Wolfe effect. If  $\delta T$  is the temperature fluctuation

$$\Omega_{\text{GW}}(f) \leq \left(\frac{H_0}{f}\right)^2 \left(\frac{\delta T}{T}\right)^2 \quad 3 \times 10^{-18} \text{Hz} < f < 10^{-16} \text{Hz}. \quad (8.4)$$

The lower frequency is fixed by demanding that the fluctuations should be inside the Hubble radius today, whereas the higher frequency by imposing that fluctuations were outside the Hubble radius at the time of the last scattering surface. Detailed analysis give [71]

$$h_0^2 \Omega_{\text{GW}}(f) \leq 7 \times 10^{-11} \left(\frac{H_0}{f}\right)^2. \quad (8.5)$$

GWs could saturate this bound if the contribution from scalar perturbations is subdominant and this depends on the specific inflationary model.

The very accurate timing of millisecond pulsars can constrain  $\Omega_{\text{GW}}$ . If a GW passes between us and the pulsar, the time of arrival of the pulse is Doppler shifted. Many years of observation yield to the bound [72] (see also Ref. [10])

$$h_0^2 \Omega_{\text{GW}} \lesssim 4.8 \times 10^{-9} \left(\frac{f}{f_*}\right)^2 \quad f > f_* = 4.4 \times 10^{-9} \text{Hz}. \quad (8.6)$$

### 8.2. Gravitational waves produced by causal mechanisms

Two features determine the typical frequency of GWs of cosmological origin produced by causal mechanism: (i) the dynamics, which is model dependent and (ii) the kinematics, i.e. the redshift from the production time. Let us assume that a graviton is produced with frequency  $f_*$  at time  $t_*$  during matter or radiation era. What is the frequency today? We have

$$f = f_* \frac{a_*}{a_0}, \quad (8.7)$$

assuming that the Universe evolved adiabatically, so  $g_S(T_*) T_*^3 a_*^3 = g_S(T_0) T_0^3 a_0^3$ , using  $T_0 = 2.73$  K and  $g_S(T_0) = 3.91$ , where  $g_S(T_*)$  is the number of degrees of freedom at temperature  $T_*$ , we get

$$f \simeq 10^{-13} f_* \left( \frac{100}{g_{S*}} \right)^{1/3} \left( \frac{1\text{GeV}}{T_*} \right). \quad (8.8)$$

What is  $f_*$ ? Since the size of the Hubble radius is the scale beyond which causal microphysics cannot operate, we can say that from causality considerations, the characteristic wavelength of gravitons produced at time  $t_*$  is  $H_*^{-1}$  or smaller. Thus, we set

$$\lambda_* = \frac{\epsilon}{H_*} \quad \epsilon \lesssim 1. \quad (8.9)$$

If the GW signal is produced during the radiation era,

$$H_*^2 = \frac{8\pi G}{3} \rho = 8\pi^3 g_* T_*^4 \frac{1}{90} \frac{1}{M_{\text{Pl}}^2}, \quad (8.10)$$

and we find

$$f \simeq 10^{-7} \frac{1}{\epsilon} \left( \frac{T_*}{1\text{GeV}} \right) \left( \frac{g_*}{100} \right)^{1/6} \text{Hz}. \quad (8.11)$$

From the above equation, we obtain that millisecond pulsars can probe physics at the  $\sim$  MeV scale, LISA at the  $\sim$  TeV scale, ground-based detectors at  $10^3$ – $10^6$  TeV and detectors in the GHz bandwidth [73] at GUT or Planck scale.

As an application of GWs produced by causal mechanisms, let us consider GW signals from first-order phase transitions. In the history of the Universe several phase transitions could have happened. The quantum-chromodynamics (QCD) phase transition takes place at  $T \sim 150$  MeV. Around  $T \sim 100$  GeV the electroweak (EW) phase transition happens (and  $SU(2) \times U(1)$  breaks to  $U_{\text{em}}(1)$  through the Higgs mechanism). Let us assume that  $V(\phi, T)$  is the potential associated to the phase transition, where  $\phi$  is the order (field) parameter. As the Universe cools down, the *true* and *false* vacuum are separated by a potential

barrier. Through quantum tunneling, bubbles of true vacuum can nucleate. The difference of energy between the true and false vacua is converted in kinetic energy (speed) of the bubble's wall. In order to start expanding, the bubbles must have the right size, so that the volume energy overcomes the shrinking effects of the surface tension. The relevant parameter is the nucleation rate  $\Gamma = \Gamma_0 e^{\beta t}$ . If  $\Gamma$  is large enough, the bubbles can collide within the Hubble radius, and being the collision nonsymmetric, they produce GWs [74]. The parameter  $\beta$  fixes the frequency at the time of production.

So, we can write for the parameter  $\epsilon$  defined in Eq. (8.9),  $\epsilon = H_*/f_* = H_*/\beta$  and the peak of the GW spectrum occurs at [75, 77, 79]

$$f_{\text{peak}} \simeq 10^{-8} \left( \frac{\beta}{H_*} \right) \left( \frac{T_*}{1\text{GeV}} \right) \left( \frac{g_*}{100} \right)^{1/6} \text{ Hz}, \quad (8.12)$$

where  $T_*$  is the temperature at which the probability that a bubble is nucleated within the horizon size is  $\mathcal{O}(1)$ .

In the case of EW phase transitions, we have  $\beta/H_* \simeq 10^2\text{--}10^3$  and  $T_* \sim 10^2$  GeV, thus  $f_{\text{peak}} \simeq 10^{-4}\text{--}10^{-3}$  Hz, which is in the frequency band of LISA. The GW spectrum can be computed semianalytically, it reads [75, 77, 79]

$$h_0^2 \Omega_{\text{GW}} \simeq 10^{-6} k^2 \frac{\alpha^2}{(1+\alpha)^2} \frac{v_b^3}{(0.24+v_b^3)} \left( \frac{H_*}{\beta} \right)^2 \left( \frac{100}{g_*} \right)^{1/3}, \quad (8.13)$$

where  $\alpha$  is the ratio between the false vacuum energy density and the energy density of the radiation at the transition temperature  $T_*$ ;  $\kappa$  quantifies the fraction of latent heat that is transformed into bubble-wall kinetic energy and  $v_b$  is the bubble expansion velocity.

Nonperturbative calculations obtained using lattice field theory have shown that there is no first-order phase transition in the standard model if the Higgs mass is larger than  $M_W$ . In minimal supersymmetric standard model, if Higgs mass is  $\sim 110\text{--}115$  GeV, the transition is first-order but  $h_0 \Omega_{\text{GW}} \sim 10^{-19}$  at  $f \sim 10$  mHz. In next-to-minimal supersymmetric standard models, there exist regions of the parameter space in which  $h_0 \Omega_{\text{GW}} \sim 10^{-15}\text{--}10^{-10}$  at  $f \sim 10$  mHz. Note that for frequencies  $10^{-4}\text{--}3 \times 10^{-3}$  Hz the stochastic GW background from white-dwarf binaries could *hide* part of the GW spectrum from first-order phase transitions. More recently, Ref. [78] pointed out that new models of EW symmetry breaking that have been proposed have typically a Higgs potential different from the one in the Standard Model. Those potentials could lead to a stronger first-order phase transition, thus to a more promising GW signature in the milliHz frequency range.

A stochastic GW background could be also produced during a first-order phase transition from turbulent (anisotropic) eddies generated in the background



fluid during the fast expansion and collision of the true-vacuum bubbles [76, 77, 79]. In the next-to-leading supersymmetric standard model there exist regions of the parameter space where [77]  $h_0^2 \Omega_{\text{GW}} \sim 10^{-10}$  with peak frequency in the mHz. Reference [80] evaluated the stochastic GW background generated by cosmic turbulence before neutrino decoupling, i.e. much later than EW phase transition, and at the end of a first-order phase transition if magnetic fields also affect the turbulent energy spectrum. The observational perspectives of those scenarios are promising for LISA.

Long time ago Turner and Wilczek [81] pointed out that if inflation ends with bubble collisions, as in extended inflation, the GW spectrum produced has a peak in the frequency range of ground-based detectors. Subsequent analyses have shown that in two-field inflationary models where a field performs the first-order phase transition and a second field provides the inflationary slow rolling (so-called first-order or false vacuum inflation [82]), if the phase transition occurs well before the end of inflation, a GW spectrum peaked around  $10\text{--}10^3$  Hz, can be produced [83], with an amplitude large enough, depending on the number of e-foldings left after the phase transition, to be detectable by ground-based interferometers. A successful detection of such a spectrum will allow to distinguish between inflation and other cosmological phase transitions, like QCD or EW, which have a different peak frequency.

Another mechanism that could have produced GWs is parametric amplification after preheating [84]. During this phase classical fluctuations produced by the oscillations of the inflaton field  $\phi$  can interact back, via parametric resonance, on the oscillating background producing GWs. In the model where the inflaton potential contains also the interaction term  $\sim \phi^2 \chi^2$ ,  $\chi$  being a scalar field, the authors of Ref. [84] estimated  $\Omega_{\text{GW}} \sim 10^{-12}$  at  $f_{\text{min}} \sim 10^5$  Hz, while in pure chaotic inflation  $\Omega_{\text{GW}} \leq 10^{-11}$  at  $f_{\text{min}} \sim 10^4$  Hz. [See Fig. 3 in Ref. [84] for the GW spectrum in the range  $10^6\text{--}10^8$  Hz and Refs. [85] for a recent reanalysis.] Unfortunately, the predictions lay in the frequency range where no GW detectors exist, but some proposals have been made [73]

### 8.3. Gravitational waves produced by cosmic and fundamental strings

Topological defects could have been produced during symmetry-breaking phase transitions in the early Universe. Since the 80s they received significant attention as possible candidates for seeding structure formation. Recently, more accurate observations of CMB inhomogeneities on smaller angular scales and compatibility with the density fluctuation spectrum on scales of  $100 h_0^{-1}$  Mpc, restrict the contribution of topological defects to less than 10%.

Cosmic strings are characterized by a single dimensional scale, the mass-per-unit length  $\mu$ . The string length is defined as the energy of the loop divided by

$\mu$ . Cosmic strings are stable against all types of decay, except from the emission of GWs. Let us assume that a network of cosmic strings did form during the evolution of the Universe. In this network the only relevant scale is the Hubble length. Small loops (smaller than Hubble radius length) oscillate, emit GWs and disappear, but they are all the time replaced by small loops broken off very long loops (longer than Hubble radius). The wavelength of the GW is determined by the length of the loop, and since in the network there are loops of all sizes, the GW spectrum is (almost) flat in a large frequency band, extending from  $f \sim 10^{-8}$  Hz to  $f \sim 10^{10}$  Hz.

In 2001, Damour and Vilenkin [86] (see also Ref. [87]), worked out that strong bursts of GWs could be produced at cusps (where the string reaches a speed very close to the light speed) and at kinks along the string loop. As a consequence of these bursts the GW background emitted by a string network is strongly non-Gaussian. The most interesting feature of these GW bursts is that they could be detectable for a large range of values of  $G\mu$ , larger than the usually considered search for the Gaussian spectrum. GW bursts can be also produced by fundamental strings, as pointed out in Ref. [88]. For a detailed analysis of the prospects of detecting the stochastic GW background and the GW bursts with ground and space-based detectors, and msec pulsars see Refs. [10, 89].

A GW burst emitted at the cusp of cosmic or fundamental strings can be detected using matched filtering. In Fourier domain the signal is [89]

$$h(f) = A|f|^{-4/3} \Theta(f_h - f) \Theta(f - f_e), \quad (8.14)$$

where  $A \sim (G\mu L^{2/3})/r$ ,  $f_e$  is determined by the size  $L$  of the feature that produces the cusp, but also by the low-frequency cutoff frequency of the detector and  $f_h \sim 2/(\theta^3 L)$ ,  $\theta$  being the angle between the line of sight and the direction of the cusp.

#### 8.4. Gravitational waves produced during inflation

The amplification of quantum vacuum fluctuations is a common mechanism in quantum field theory in curved space time [90]. In the 70s Grishchuk and Starobinsky [91] applied it to cosmology, predicting a stochastic GW background which today would span a very large frequency band  $10^{-17}$ – $10^{10}$  Hz. Henceforth, we shall compute the GW spectrum using semiclassical arguments, and refer the reader to Refs. [92, 93] for more detailed computations.

The background field dynamics is described by the action

$$S = \frac{1}{16\pi G} \int d^4x \sqrt{-g} R + S_m. \quad (8.15)$$

We assume an isotropic and spatially homogeneous Friedmann- Lamaitre-Robertson-Walker metric with scale factor  $a$ ,

$$ds^2 = -dt^2 + a^2 d\mathbf{x}^2 = g_{\mu\nu} dx^\mu dx^\nu. \quad (8.16)$$

For what we have learned in previous lectures, we can derive the free-linearized wave equations for the TT metric perturbations  $\delta g_{\mu\nu} = h_{\mu\nu}$ , with  $h_{\mu 0} = 0$ ,  $h_{\mu}^{\mu} = 0$ ,  $h_{\nu;\mu}^{\mu} = 0$  and  $\delta T_{\mu}^{\nu} = 0$ , obtaining

$$\square h_i^j = \frac{1}{\sqrt{-g}} \partial_{\mu} (\sqrt{-g} g^{\mu\nu} \partial_{\nu}) h_i^j = 0, \quad (8.17)$$

where we disregard any anisotropic stresses. Introducing the conformal time  $\eta$ , with  $d\eta = dt/a(t)$ , we can write

$$h_i^j(\eta, \mathbf{x}) = \sqrt{8\pi G} \sum_{A=+, \times} \sum_{\mathbf{k}} h_{\mathbf{k}}^A(\eta) e^{i\mathbf{k}\cdot\mathbf{x}} e_i^{Aj}(\mathbf{n}), \quad (8.18)$$

$e_i^{Aj}(\mathbf{n})$  being the polarization tensors. Since we assume isotropic and spatially homogeneous metric perturbations  $h_{\mathbf{k}} = h_k$ , and each polarization mode satisfies the equation

$$h_k''(\eta) + 2\frac{a'}{a} h_k'(\eta) + k^2 h_k(\eta) = 0, \quad (8.19)$$

where we denote with a prime the derivative with respect to the conformal time. By introducing the canonical variable  $\psi_k(\eta) = a h_k(\eta)$  we can recast Eq. (8.19) in the much simpler form

$$\psi_k''(\eta) + [k^2 - U(\eta)] \psi_k = 0, \quad U(\eta) = \frac{a''}{a}, \quad (8.20)$$

which is the equation of an harmonic oscillator in a time-depedent potential  $U(\eta)$ . We want to solve the above equation and study the properties of the solutions.

For simplicity, we consider a De Sitter inflationary era,  $a = -1/(H_{\text{DS}} \eta)$  and  $a''/a = 2/\eta^2$ , and make the crude assumption that the De Sitter era is followed instantaneously by the radiation era,  $a(\eta) = (\eta - 2\eta_*)/(H_{\text{DS}} \eta_*^2)$  and  $a''(\eta) = 0$ .

If  $k^2 \gg U(\eta)$ , i.e.  $k\eta \gg 1$  or  $a/k \ll |a\eta| = H_{\text{DS}}^{-1}$ , the mode is inside the Hubble radius or (in jargon) is over the potential barrier  $U(\eta)$  and the (positive frequency) solution reads

$$\psi_k \sim \frac{1}{\sqrt{2k}} e^{-ik\eta} \quad \Rightarrow \quad h_k \sim \frac{1}{2k} \frac{1}{a} e^{-ik\eta}, \quad (8.21)$$

thus  $h_k$  decreases while inside the Hubble radius. If  $k^2 \ll U(\eta)$ , i.e.  $k\eta \ll 1$ ,  $a/k \gg |a\eta| = H_{\text{DS}}^{-1}$ , the mode is outside the Hubble radius or (in jargon) under the potential barrier. In this case the solution reads

$$\psi_k \sim a \left[ A_k + B_k \int \frac{d\eta}{a^2(\eta)} \right] \Rightarrow h_k \sim A_k + B_k \int \frac{d\eta}{a^2(\eta)}. \quad (8.22)$$

Since during the De Sitter era the scale factor gets larger and larger, the term proportional to B in the above equation becomes more and more negligible. Thus, the perturbation  $h_k$  remains (almost) constant while outside the Hubble radius. So, the longer the tensorial-perturbation mode remains outside the Hubble radius, the more it gets amplified (with respect to the case it stayed always inside the Hubble radius). During the RD era, the mode is again under the barrier, and the solution is

$$\psi_k = \alpha_k e^{-ik\eta} + \beta_k e^{+ik\eta}, \quad (8.23)$$

and contains both positive and negative modes. Even normalizing the initial state to positive frequency mode, the final state is a mixture of positive and frequency modes. In a quantum field theory language, such a mixing represents a process of pair production from vacuum. The coefficients  $\alpha_k$  and  $\beta_k$  are called Bogoliubov coefficients and can be obtained imposing the continuity of the tensorial perturbation and its first time derivative at the transition between cosmological phases.

The intensity of the stochastic GW background can be expressed in terms of the number of gravitons per cell of the phase space  $n_f$  with  $f = |\mathbf{k}|/(2\pi)$ . For an isotropic stochastic GW background  $\rho_{\text{GW}} = 2 \int d^3k/(2\pi)^3 (k n_k)$ , thus

$$\Omega_{\text{GW}}(f) = \frac{1}{\rho_c} 16\pi^2 n_f f^4. \quad (8.24)$$

where  $n_f = |\beta_f|^2$ .

The stochastic GW spectrum produced during *slow-roll* inflation, decreases as  $f^{-2}$  in the frequency window  $10^{-18}$ – $10^{-16}$  Hz, and then slowly decreases up to a frequency corresponding to modes whose physical frequency becomes less than the maximum causal distance during the reheating phase (which is of order of a few GHz). Its magnitude depends on both the value of the Hubble parameter during inflation and a number of features characterizing the Universe evolution after the inflationary era — for example tensor anisotropic stress due to free-streaming relativistic particles, equations of state, etc. [93, 94]. An upper bound on the spectrum can be obtained from the measurement of the quadrupole anisotropy of the CMB, as seen in Sec. 8.1. Since for a generic slow-roll inflationary model the spectrum is (weakly) decreasing with frequency this implies an

upper bound  $h_0^2 \Omega_{\text{GW}} \sim 5 \times 10^{-16}$  at frequencies around  $f \sim 100$  Hz, where ground-based detectors reach the best sensitivity. The spectrum predicted by the class of single-field inflationary models is then too low to be observed by ground-based and also space-based detectors. It is therefore evident that a background satisfying the bound imposed by the observed amount of CMB anisotropies at large scales could be detected by GW interferometers provided that its spectrum grows significantly with frequency. This could happen in bouncing Universe cosmologies, such as pre-big-bang scenario [95, 96], the ekpyrotic models [97] (although the amplitude of the GW spectrum is too low to be observable) and in quintessential inflation [98].

Finally, a stochastic GW background can be detected by correlating two GW interferometers [99]. The upper limit on a flat-spectrum set by the LIGO Scientific Collaboration is  $h_0^2 \Omega_{\text{GW}} \simeq 6.5 \times 10^{-5}$  in the frequency band 70–156 Hz [28]. For frequency-independent spectra, the expected upper limit for the current LIGO configuration is  $h_0^2 \Omega_{\text{GW}} < 5 \times 10^{-6}$ , while for advanced LIGO project is  $h_0^2 \Omega_{\text{GW}} \sim 8 \times 10^{-9}$ .

## 9. Acknowledgments

I wish to thank the organizers of the Les Houches School for having invited me to such a pleasant and stimulating school and all the students for their interesting questions. I acknowledge support from NSF grant PHY-0603762 and from the Alfred Sloan Foundation. I wish to thank also Francis Bernardeau and Christophe Grojean for their patience.

## References

- [1] A. Abramovici et al., *Science* **256**, 325 (1992); <http://www.ligo.org>
- [2] B. Caron et al., *Class. Quant. Grav.* **14**, 1461 (1997); <http://www.virgo.infn.it>
- [3] H. Lück et al., *Class. Quant. Grav.* **14**, 1471 (1997); <http://www.geo600.uni-hannover.de>
- [4] M. Ando et al., *Phys. Rev. Lett.* **86**, 3950 (2001); <http://tamago.mtk.nao.ac.jp>
- [5] B.J. Meers and K. Strain, *Phys. Rev. A* **44**, 4693 (1991); J. Mizuno et al., *Phys. Lett. A* **175**, 273 (1993); A. Buonanno and Y. Chen, *Phys. Rev. D* **64**, 042006 (2001).
- [6] V.B. Braginsky and F.Ya. Khalili, *Phys. Lett. A* **147**, 251 (1990); V.B. Braginsky, M.L. Gorodetsky, F.Ya. Khalili, and K.S. Thorne, *Phys. Rev. A* **61**, 044002 (2000); P. Purdue, *Phys. Rev. D* **66**, 022001 (2001); P. Purdue and Y. Chen, *Phys. Rev. D* **66**, 122004 (2002); J. Harms et al. *Phys. Rev. D* **68**, 042001 (2003); ; A. Buonanno and Y. Chen, *Phys. Rev. D* **69** 102004 (2004).
- [7] <http://www.lisa-science.org>
- [8] P. Astone et al., *Europhys. Lett.* **12**, 5 (1990); G. Pallottino, in “Gravitational Waves, Sources and Detectors,” p 159 (Singapore, World Scientific, 1997); E. Mauceli et al., *Phys. Rev.* **D54**,

- 1264 (1996); D. Blair et al., Phys. Rev. Lett. **74**, 1908 (1995); M. Cerdonio et al., Class. Quantum Grav. **14**, 1491 (1997).
- [9] M. Kamionkowski, A. Kosowsky, and A. Stebbins, Phys. Rev. **D55**, 7368 (1997); U. Seljak and M. Zaldarriaga, Phys. Rev. **D78**, 2054 (1997); M. Kamionkowski and A. Kosowsky, Phys. Rev. **D57**, 685 (1998).
- [10] See, e.g., F.A. Jenet et al., Astrophys. J. **653**, 1571 (2006), and references therein.
- [11] <http://www.skatelescope.org>
- [12] T. Damour, *The problem of motion in Newtonian and Einsteinian gravity*, in *300 Years of Gravitation* ed. by S.W. Hawking and W. Israel (Cambridge University Press, Cambridge, 1987).
- [13] P. Jaranowski, and G. Schäfer, Phys. Rev. D **57**, 7274 (1998); Erratum-ibid D **63** 029902; T. Damour, P. Jaranowski, and G. Schäfer, Phys. Lett. B **513**, 147 (2001); L. Blanchet, G. Faye, B.R. Iyer, and B. Joguet, Phys. Rev. D **65**, 061501(R) (2002); Erratum-ibid D **71**, 129902 (2005); L. Blanchet, T. Damour, G. Esposito-Farese, and B.R. Iyer, Phys. Rev. Lett. **93**, 091101 (2004).
- [14] See, e.g., L. Blanchet, Living Rev. Rel. **5**, 3 (2002) and references therein. <http://relativity.livingreviews.org>
- [15] L. Kidder, C. Will, and A. Wiseman, Phys. Rev. D **47**, 4183 (1993). L. Kidder, Phys. Rev. D **52**, 821 (1995). B. Owen, H. Tagoshi, and Ohashi, Phys. Rev. D **57**, 6168 (1998). H. Tagoshi, Ohashi, and B. Owen, Phys. Rev. D **63**, 044006 (2001). G. Faye, L. Blanchet, and A. Buonanno, Phys. Rev. D **74**, 104033 (2006); L. Blanchet, A. Buonanno, and G. Faye, Phys. Rev. D **74**, 104034 (2006).
- [16] A. Buonanno and T. Damour, Phys. Rev. D **59**, 084006 (1999); *ibid.* D **62**, 064015 (2000); A. Buonanno and T. Damour, Proceedings of IX<sup>th</sup> Marcel Grossmann Meeting (Rome, July 2000) [gr-qc/0011052]; T. Damour, P. Jaranowski, and G. Schäfer, Phys. Rev. D **62**, 084011 (2000); T. Damour, Phys. Rev. D **64**, 124013 (2001); A. Buonanno, Y. Chen, and T. Damour, Phys. Rev. D **74**, 104005 (2006).
- [17] T. Damour, B.R. Iyer, and B.S. Sathyaprakash, Phys. Rev. D **57**, 885 (1998).
- [18] W.D. Goldberger and I.Z. Rothstein, Phys. Rev. D **73**, 104029 (2006); R.A. Porto, Phys. Rev. D **73**, 104031 (2006); R.A. Porto and I.Z. Rothstein, Phys. Rev. Lett. **97**, 021101 (2006).
- [19] F. Pretorius, Phys. Rev. Lett. **95**, 121101 (2005); M. Campanelli, C.O. Lousto, P. Marronetti, and Y. Zlochower, Phys. Rev. Lett. **96**, 111101 (2006); J. Baker, J. Centrella, D. Choi, M. Koppitz, and J. van Meter, Phys. Rev. Lett. **96**, 111102 (2006).
- [20] See, e.g., E. Poisson, Living Rev. Rel. **6**, 3 (2004), and references therein. <http://relativity.livingreviews.org>
- [21] Y. Mino, Prog. Theor. Phys. **113**, 733 (2005); *ibid.* Prog. Theor. Phys. **115**, 43 (2006); A. Pound, E. Poisson, and B.G. Nickel, Phys. Rev. D **72**, 124001 (2005); L. Barack and C. Lousto, Phys. Rev. D **72**, 104026 (2005); L. Barack and N. Sago, Phys. Rev. D **75**, 064021 (2007).
- [22] L. S. Finn and K. S. Thorne, Phys. Rev. D **62**, 124021 (2000); S. Babak et al. Phys. Rev. D **75**, 024005 (2007); L. Barack and C. Cutler, Phys. Rev. D **70**, 122002 (2004); *ibid.* Phys. Rev. D **70**, 122002 (2004); G. Sigl, J. Schnittman, and A. Buonanno, Phys. Rev. D **75**, 024034 (2007).
- [23] C. Cutler et al., Phys. Rev. Lett. **70**, 2984 (1993); T. Damour, B. Iyer, and B. Sathyaprakash, Phys. Rev. D **63**, 044023 (2001); *ibid.* D **66**, 027502 (2002); T. Damour, B.R. Iyer, and B.S. Sathyaprakash, Phys. Rev. D **67**, 064028 (2003); A. Buonanno, Y. Chen, and M. Vallisneri, Phys. Rev. D **67**, 104025 (2003); Erratum-*ibid.* D **74**, 029904 (2006); A. Buonanno, Y. Chen, and M. Vallisneri, Phys. Rev. D **67**, 024016 (2003); Erratum-*ibid.* D **74**, 029903 (2006); T. Damour, B. Iyer, P. Jaranowski, and B. Sathyaprakash, Phys. Rev. D **67**, 064028 (2003); A. Buonanno, Y. Chen, and M. Vallisneri, Phys. Rev. D **67**, 104025 (2003); Erratum-*ibid.* D **74**, 029904 (2006); Y. Pan, A. Buonanno, Y. Chen and M. Vallisneri, Phys. Rev. D **69** 104017 (2004).

- [24] L.S. Finn, Phys. Rev. D **46**, 5236 (1992); L. S. Finn and D.F. Chernoff, Phys. Rev. D **47**, 2198 (1993); É.E. Flanagan and S.A. Hughes, Phys. Rev. D **57**, 4535 (1998).
- [25] P.R. Brady, T. Creighton, C. Cutler, and B.F. Schutz, Phys. Rev. D **57**, 2101 (1998); P.R. Brady and T. Creighton, Phys. Rev. D **61**, 082001 (2000); M. Tinto, F.B. Estabrook, and J.W. Armstrong, Phys. Rev. D **65**, 082003 (2002); B. Krishnan et al. Phys. Rev. D **70**, 082001 (2004); C. Cutler, I. Gholami, and B. Krishnan, Phys. Rev. D **72**, 042004 (2005); S. Chatterji et al., Phys. Rev. D **74**, 082005 (2006).
- [26] B. Abbott et al. (LIGO Scientific Collaboration), Phys. Rev. D **72** 082002 (2005); *ibid.* D **72** 122004 (2005); *ibid.* D **72** 102004 (2005); *ibid.* D **73** 062001 (2006); *ibid.* D **73** 102002 (2006).
- [27] B. Abbott et al. (LIGO Scientific Collaboration), *Coherent searches for periodic gravitational waves from unknown isolated sources and Scorpius X-1*, [gr-qc/0605028].
- [28] B. Abbott et al. (LIGO Scientific Collaboration), Phys. Rev. Lett. **95** 221101 (2005); *Searching for a stochastic background of gravitational waves with LIGO*, [astro-ph/0608606].
- [29] L.D. Landau and E.M. Lifshits, *The Classical Theory of Field*, (Pergamon Press, Oxford, 1975).
- [30] C. Misner, K.S. Thorne, and J.A. Wheeler, *Gravitation* (W.H. Freeman and Company, New York, 1973).
- [31] S. Weinberg, *Gravitation and cosmology* (John Wiley and Sons, New York, 1972).
- [32] R.M. Wald, *General relativity* (The University of Chicago Press, Chicago, 1983)
- [33] B. Schutz, *A first course in general relativity* (Cambridge University Press, Cambridge, 1985).
- [34] S. Carroll *Spacetime and geometry: an introduction to general relativity* (Addison-Wesley, 2003).
- [35] M. Maggiore, *Gravitational waves: Theory and Experiments* (Oxford University Press, Oxford, 2007).
- [36] K.S. Thorne, *Gravitational radiation*, in *300 Years of Gravitation* ed. by S.W. Hawking and W. Israel (Cambridge University Press, Cambridge, 1987).
- [37] B. Allen, *Lectures at Les Houches School* (1996) [gr-qc/9604033].
- [38] M. Maggiore, Phys. Rep. **331**, 283 (2000).
- [39] C. Cutler and K.S. Thorne, *An overview of gravitational-wave sources* (2002) [gr-qc/0204090] and references therein.
- [40] A. Buonanno, *TASI lectures on gravitational-wave from the early Universe* (2003) [gr-qc/0303085].
- [41] É.E. Flanagan and S.A. Hughes, *The basics of gravitational-wave theory*, New J.Phys. **7**, 204 (2005).
- [42] K.S. Thorne, <http://elmer.caltech.edu/ph237/>
- [43] A. Einstein, Sitzber. Preuss. Akad. Wiss., 688 (1916); see also Preuss. Akad. Wiss., 154 (1918).
- [44] W.T. Ni and M. Zimmermann, Phys. Rev. D **17**, 1473 (1978).
- [45] M. Rakhmanov, Phys. Rev. D **71**, 084003 (2005).
- [46] D.R. Brill and J.B. Hartle, Phys. Rev. **135**, B271 (1963). R.A. Isaacson, Phys. Rev. **166**, 1263 (1968); **166**, 1272 (1968).
- [47] M. Walker and C.M. Will, Astrophys. J. **242**, L129 (1980); M. Walker and C.M. Will, Phys. Rev. Lett. **45**, 1741 (1980); T. Damour, Phys. Rev. Lett. **51**, 1019 (1983);
- [48] F. Herrmann, D. Shoemaker, and P. Laguna, [gr-qc/0601026]; J.G. Baker, J. Centrella, D. Choi, M. Koppitz, J. R. van Meter, and M.C Miller, Astrophys. J **653**, L93 (2006); M. Campanelli, C.O. Lousto, and Y. Zlochower, Phys. Rev. D **74**, 041501 (2006); *ibid.* D **74**, 084023 (2006); U. Sperhake, [gr-qc/0606079]; J. A. Gonzalez, U. Sperhake, B. Bruegmann, M. Hannam, and S. Husa, Phys.Rev.Lett.**98**,091101 (2007); M. Koppitz, D. Pollney, C. Reisswig, L. Rezzolla, J.



- Thornburg, P. Diener, and E. Schnetter, [gr-qc/0701163]; M. Campanelli, C.O. Lousto, Y. Zlochower, and D. Merritt, [gr-qc/0701164]; F. Herrmann, I. Hinder, D. Shoemaker, P. Laguna, and R. A. Matzner [gr-qc/0701143]; J.A. Gonzalez, M.D. Hannam, U. Sperhake, B. Bruggmann, and S. Husa, [gr-qc/0702052]; J.G. Baker, W.D. Boggs, J. Centrella, B.J. Kelly, S.T. McWilliams, M. C. Miller, and J.R. van Meter, [astro-ph/0702390]; W. Tichy and P. Marronetti, [gr-qc/0703075];
- [49] L. Blanchet, M.S.S. Qusailah, and C.M. Will, *Astrophys. J.* **635**, 508 (2006); T. Damour and A. Gopakumar, *Phys. Rev. D* **73**, 124006 (2006); C.F. Sopuerta, N. Yunes, and P. Laguna (2006) [astro-ph/0611110]; J. Schnittman and A. Buonanno (2007), [astro-ph/0702641].
- [50] H. Bondi, *Nature* **179**, 1072 (1957); *ibid.* **186**, 535 (1960).
- [51] P.C. Peters and J. Mathews, *Phys. Rev.* **131**, 435 (1963); P.C. Peters, *Phys. Rev.* **136**, B1224 (1964).
- [52] R. Hulse and J. Taylor, *Astrophys. J.*, **324** (1975).
- [53] C.V. Vishveshwara, *Nature* **227**, 936 (1970); B. Schutz and C.M. Will, *Astrophys. J.* **291**, 33 (1985); S. Chandrasekhar and S. Detweiler, *Proc. R. Soc. Lond. A* **344**, (1975) 441; B. Mashhoon, *Phys. Rev. D* **31**, 290 (2005).
- [54] W. Press, *Astrophys J. Letters* **170**, L105 (1971).
- [55] M. Davis, R. Ruffini, W.H. Press, and R.H. Price, *Phys. Rev. Lett.* **27**, 1466 (1971); M. Davis, R. Ruffini, and J. Tiomno, *Phys. Rev. D* **5**, 2932 (1972).
- [56] R.H. Price and J. Pullin, *Phys. Rev. Lett.* **72**, 3297 (1994); A. M. Abraham and G.B. Cook, *Phys. Rev. D* **50**, R2364 (1994); R.J. Gleiser, C.O. Nicasio, R. Price, and J. Pullin, *Class. Quant. Grav.* **13**, L117 (1996); *Phys. Rev. Lett.* **77**, 4483 (1996); J. Pullin, *The close limit of colliding black holes: an update*, Talk given at the Yukawa International Symposium at Kyoto, Japan, 1999 [gr-qc/9909021] and references therein; P. Anninos, D. Hobill, E. Seidel, L. Smarr, and W.M. Suen, *Phys. Rev. Lett.* **71**, 2851 (1993); Z. Andrade and R. H. Price, *Phys.Rev.D* **56**, 6336 (1997); J. Baker, A. Abrahams, P. Anninos, S. Brandt, R. Price, J. Pullin and E. Seidel, *Phys. Rev. D* **55**, 829 (1997).
- [57] J. Baker, B. Brügmann, M. Campanelli, C.O. Lousto, and R. Takahashi, *Phys. Rev. Lett.* **87**, 121103 (2001).
- [58] A. Buonanno, G. Cook, and F. Pretorius (2006), [gr-qc/0610122].
- [59] J. Baker, J. van Meter, S. McWilliams, J. Centrella, and B. Kelly (2006), [gr-qc/0612024].
- [60] C. Cutler and É.E. Flanagan, *Phys. Rev. D* **49**, 2658 (1994); A. Krolak, K. D. Kokkotas, and G. Schafer, *Phys. Rev. D* **52**, 2089 (1995); E. Poisson and C.M. Will, *Phys. Rev. D* **52**, 848 (1995); Arun et al., *Phys. Rev. D* **71**, 084008 (2005); Erratum-*ibid.* **72**, 069903 (2005).
- [61] C.M. Will, *Phys. Rev. D* **50**, 6058 (1994); C.M. Will, *Phys. Rev. D* **57**, 2061 (1998); T. Damour and G. Esposito-Farèse, *Phys. Rev. D* **58**, 042001 (1998); P.D. Scharre and C.M. Will, *Phys. Rev. D* **65**, 042002 (2002); C.M. Will and N. Yunes, *Class. Quantum Gravit.* **21**, 4367 (2004);
- [62] E. Berti, A. Buonanno, and C.S. Will, *Phys. Rev. D* **71** 084025 (2005).
- [63] B.J. Owen, *Phys. Rev. Lett.* **95**, 211101 (2005).
- [64] M. Zimmermann and E. Szedenis, *Phys. Rev. D* **20**, 351 (1979); M. Zimmermann and E. Szedenis, *Phys. Rev. D* **21**, 891 (1980); C. Cutler and D.I. Jones, *Phys. Rev.D* **63**, 024002 (2001).
- [65] H. Dimmelmeier, J. A. Font, and E. Mueller, *Astron. Astrophys.* **393**, 523 (2002); E. Müller, M. Rampp, R. Buras, H.-T. Janka, and D. H. Shoemaker, *Astrophys. J.* **603**, 221 (2004); C. L. Fryer, D. E. Holz, and S. A. Hughes, *Astrophys. J.* **609**, 288 (2004); A. Burrows et al., *Astrophys. J.* **640**, 878 (2006); H. Dimmelmeier et al., [astro-ph/0702305].
- [66] A. Buonanno, G. Sigl, G. Raffelt, T. Janka, and E. Mueller, *Phys. Rev. D* **72** 084001 (2005).
- [67] S. Kobayashi and P. Meszaros, *Astrophys. J.* **589**, 861 (2003).
- [68] A.J. Farmer and E.S. Phinney, *Mon. Not. Roy. Astron. Soc.* **346**, 1197 (2003).



- [69] C.J. Copi, D.N. Schramm, and M.S. Turner, Phys. Rev. **D55**, 3389 (1997).
- [70] T. L. Smith, E. Pierpaoli, and M. Kamionkowski, Phys. Rev. Lett. **97**, 021301 (2006).
- [71] B. Allen and S. Koranda, Phys. Rev. **D50**, 3713 (1994).
- [72] S. Thorsett and R. Dewey, Phys. Rev. **D53**, 3468 (1996).
- [73] V.B. Braginski, L.P. Grishchuck, A.G. Doroshkevich, Ya.B. Zeldovich, I.D. Novikov and M.V. Sazhin, Sov. Phys. JETP **38**, 865 (1974); E. Iacopini, E. Picasso, F. Pegoraro, and L.A. Radicati, Phys. Lett **73A**, 140 (1979); C.M. Caves, Phys. Lett. **80B**, 323 (1979).
- [74] C.J. Hogan, Phys. Lett. **B133**, 172 (1983); E. Witten, Phys. Rev. **D30**, 272 (1984); C.J. Hogan, Mon. Not. R. Astr. Soc. **218**, 629 (1986).
- [75] A. Kosowsky, M.S. Turner, and R. Watkins, Phys. Rev. **D45**, 4514 (1992); Phys. Rev. Lett. **69**, 2026 (1992); A. Kosowsky and M.S. Turner, Phys. Rev. **D47**, 4372 (1993); M. Kamionkowski, A. Kosowsky, and M.S. Turner, Phys. Rev. **D49**, 2837 (1994).
- [76] See M. Kamionkowski, A. Kosowsky, and M.S. Turner in Ref. [75].
- [77] R. Apreda, M. Maggiore, A. Nicolis, and A. Riotto, Class. Quant. Grav. **18**, L155-L162 (2001); Nucl. Phys. **B631**, 342 (2002); A. Nicolis, PhD Thesis 2002, Scuola Normale Superiore, Pisa, Italy.
- [78] C. Grojean and G. Servant, Phys. Rev. D **75**, 043507 (2007).
- [79] A. Kosowsky, A. Mack, and T. Kahniashvili, Phys. Rev. **D66**, 024030 (2002).
- [80] A.D. Dolgov and D. Grasso, Phys. Rev. Lett. **88**, 011301 (2002); A.D. Dolgov, D. Grasso, and A. Nicolis, Phys. Rev. **D66**, 103505 (2002).
- [81] M.S. Turner and F. Wilczek, Phys. Rev. Lett **65**, 3080 (1990).
- [82] See, e.g., M.S. Turner, E.J. Weinberg, and L.M. Widrow, Phys. Rev. **D46**, 2384 (1992); E.J. Copeland, A.R. Liddle, D.H. Lyth, E.D. Stewart, and D. Wands, Phys. Rev. **D49**, 6410 (1994).
- [83] C. Baccigalupi, L. Amendola, P. Fortini, and F. Occhionero, Phys. Rev. **D56**, 4610 (1997).
- [84] S. Khlebnikov and I. Tkachev, Phys. Rev. **D56**, 653 (1997).
- [85] R. Easther, J.T. Giblin, and E.A. Lim, [astro-ph/0612294]; J. Garcia-Bellido and D. G. Figueroa, Phys. Rev. Lett. **98**, 061302 (2007).
- [86] T. Damour and A. Vilenkin, Phys. Rev. Lett. **85**, 3761 (2000); Phys. Rev. **D64**, 064008 (2001); *ibid.* Phys. Rev. D **71**, 063510 (2005).
- [87] V. Berezhinsky, B. Hnatyk, and A. Vilenkin, [astro-ph/0001213].
- [88] E.J. Copeland, R.C. Myers, and J. Polchinski, JHEP **0406**, 013 (2004); M. G. Jackson, N.T. Jones, and J. Polchinski, JHEP **0510**, 013 (2005); J. Polchinski, [hep-th/0410082].
- [89] X. Siemens et al., Phys. Rev. D **73**, 105001 (2006); X. Siemens, V. Mandic, and J. Creighton, Phys. Rev. Lett. **98**, 111101 (2007).
- [90] N.D. Birrell and P.C.W. Davis, *Quantum fields in curved space*, (Cambridge, Cambridge University Press, 1982).
- [91] L. Grishchuk, Sov. Phys. JETP **40**, 409 (1974); A. Starobinsky, JETP Lett. **30**, 682 (1979); L. Grishchuk Class. Quantum Grav. **10**, 2449 (1993).
- [92] L.F. Abbott and D.D. Harari, Nucl. Phys. **B264**, 487 (1986); B. Allen, Phys. Rev. **D37**, 2078 (1988); V. Sahni, Phys. Rev. **D42**, 453 (1990); M. S. Turner, Phys. Rev. **D55**, R435 (1996); L. Krauss and M. White, Phys. Rev. Lett. **69**, 869 (1992); L. Hui and W.H. Kinney, Phys. Rev. **D65**, 103507 (2002).
- [93] L. Boyle, P. Steinhardt, and N. Turok, Phys. Rev. Lett. **96**, 111301 (2006); L. Boyle and P. Steinhardt, [astro-ph/0512014]; T. Smith, A. Cooray, and M. Kamionkowski, Phys. Rev. D **73**, 023504 (2006).
- [94] S. Weinberg, Phys. Rev. D **69**, 023503 (2004).

- [95] M. Gasperini and G. Veneziano, *Phys. Rep.* **373**, 1 (2003).
- [96] R. Brustein, G. Gasperini, G. Giovannini, and G. Veneziano, *Phys. Lett.* **B361**, 45 (1995); M. Gasperini, [hep-th/9604084]; A. Buonanno, M. Maggiore, and C. Ungarelli, *Phys. Rev.* **D55**, 3330 (1997); M. Gasperini, *Phys. Rev.* **D56**, 4815 (1997); A. Buonanno, K. Meissner, C. Ungarelli, and G. Veneziano, *JHEP* **001**, 004 (1998).
- [97] J. Khoury, B.A. Ovrut, P.J. Steinhardt, and N. Turok, *Phys. Rev.* **D64**, 123522 (2001); J. Khoury, B.A. Ovrut, N. Seiberg, P.J. Steinhardt, and N. Turok, *Phys. Rev.* **D65**, 086007 (2002); L. Boyle, P. Steinhardt, and N. Turok, *Phys. Rev. D* **69**, 127302 (2004)
- [98] P.J.E. Peebles and A. Vilenkin, *Phys. Rev.* **D59**, 063505 (1999); M. Giovannini, *Phys. Rev.* **D60**, 123511 (1999).
- [99] N. Christensen, *Phys. Rev.* **D46**, 5250 (1992); É.E. Flanagan, *Phys. Rev.* **D48**, 2389 (1993); B. Allen and J.D. Romano, *Phys. Rev.* **D59**, 102001 (1999); S. Drasco and E. E. Flanagan, *Phys. Rev. D* **67**, 082003 (2003).